

## Article

# Non-Invasive On-Site pXRF Analysis of Coloring Agents, Marks and Enamels of Qing Imperial and Non-Imperial Porcelain

Philippe Colomban <sup>1,\*</sup> , Gulsu Simsek Franci <sup>2</sup> , Jacques Burlot <sup>1</sup> , Xavier Gallet <sup>3</sup>, Bing Zhao <sup>4</sup> and Jean-Baptiste Clais <sup>5</sup>

<sup>1</sup> MONARIS UMR8233, Sorbonne Université, CNRS, 4 Place Jussieu, 75005 Paris, France

<sup>2</sup> Surface Science and Technology Center (KUYTAM), College of Sciences, Rumelifeneri Campus, Koç University, 34450 Istanbul, Turkey

<sup>3</sup> UMR 7194—Histoire Naturelle de l'Homme Préhistorique (HNHP), Musée National d'Histoire Naturelle, CNRS, Université Perpignan Via Domitia, Musée de l'Homme, 17 Place du Trocadéro, 75116 Paris, France

<sup>4</sup> CNRS, CRCAO, UMR8155, Collège de France, 75005 Paris, France

<sup>5</sup> Département des Objets d'art, Musée du Louvre, Quai François Mitterrand, 75001 Paris, France

\* Correspondence: philippe.colomban@sorbonne-universite.fr or philippe.colomban@upmc.fr

**Abstract:** On-site pXRF analysis in various French collections (Musée du Louvre, Musée national des Arts asiatiques-Guimet, Paris) of porcelains decorated with painted enamels from the Qing Dynasty, in particular porcelains bearing an imperial mark, identifies the types of enamels/glazes, the ions and coloring phases or the opacifier. The study of the elements associated with cobalt (nickel, manganese, arsenic, etc.) and of the impurities of the silicate matrix (yttrium, rubidium and strontium) differentiates the use of 'Chinese/Asian' raw materials from ones imported from Europe by the initiative of the European missionaries (chiefly Jesuits) present at the Court (Beijing). Particular attention is paid to the analysis of the blue color of the marks and to the elements associated with the use of gold or copper nanoparticles as well as to the compositions of the pyrochlore phases (tin yellow, Naples yellow). The comparison is extended to pXRF and Raman microspectroscopy measurements previously made on other Qing imperial porcelains as well as on Cantonese productions (on porcelain or metal) from different Swiss and French museums and blue-and-white wares of the Ming and Yuan Dynasties (archaeological and private collections).

**Keywords:** pXRF; porcelain; enamels; glaze; cobalt; arsenic; gold; mark; pigments; opacifier; blue; yellow; green; rose; red; white



**Citation:** Colomban, P.; Simsek Franci, G.; Burlot, J.; Gallet, X.; Zhao, B.; Clais, J.-B. Non-Invasive On-Site pXRF Analysis of Coloring Agents, Marks and Enamels of Qing Imperial and Non-Imperial Porcelain. *Ceramics* **2023**, *6*, 447–474. <https://doi.org/10.3390/ceramics6010026>

Academic Editor:  
Frederic Monteverde

Received: 30 December 2022

Revised: 21 January 2023

Accepted: 28 January 2023

Published: 3 February 2023



**Copyright:** © 2023 by the authors. Licensee MDPI, Basel, Switzerland. This article is an open access article distributed under the terms and conditions of the Creative Commons Attribution (CC BY) license (<https://creativecommons.org/licenses/by/4.0/>).

## 1. Introduction

The techniques for coloring a layer of glass implement with three types of coloring agents: (i) Ions exhibiting absorption in the visible, i.e., having an incomplete 3d electronic shell (transition metals) or 4f (rare earths) dissolved in the silicate network; (ii) nanoparticles absorbing in the visible, i.e., low-band gap (metals such as gold, copper or silver and semiconductors such as CdS and CdSe); (iii) pigments colored by the means mentioned above, prepared separately and dispersed in the silicate powder before firing or forming on cooling from the silicate melt oversaturated in certain elements [1–4]. The technical literature shows that, for the same visual aspect, several preparation techniques are possible [1–6]. For a long time, most of the colored glazes and enamels were prepared from two mixtures: One enriched in coloring agent(s) (e.g., smalt, the cobalt-rich potash glass that contain up to ~20 wt% CoO [6]), called *anima* in ancient recipes [7] and a colorless mixture (*corpo*) that will form the silicate matrix [1,8], convenient for the control of the melting temperature, the thermal expansion and the viscosity, etc. [2,9]. The first mixture, and rarely the second one, is prepared by the glass technique: Raw materials are melted

in a crucible and the melt is poured in water, which leads to the reduction of the glass to a powder called *frit*. Typically, the content of the coloring phase ranges from less than 0.5 wt% (e.g., CoO or Au<sup>0</sup>) up to 5–10 wt% (e.g., Fe<sub>2</sub>O<sub>3</sub> and opacifiers).

In this work, we will compare a selection of painted enameled objects, mainly porcelain, belonging to the collections of the Musée national des Arts asiatiques-Guimet (mnaa-G) and the Musée du Louvre bearing imperial marks and/or stylistically attributed to the reigns of Kangxi, Yongzheng and Qianlong Emperors. Most of these objects have already been analyzed by Raman microspectroscopy [10–13]. Additional artifacts assigned to the second part of the 19th century are also studied for comparison. Painted enamel decorations, as opposed to ceramics decorated under glaze (typically blue-and-white porcelain) and by monochrome enamels or made by nearly homogeneous colored areas are particularly complex because, to represent sophisticated compositions as in oil painting, the glazes must be heterogeneous at different scales (overlay of layers, distribution of pigments and coloring agents). We will then compare the results with those obtained on similar pieces from the Chinese museum of the Château de Fontainebleau [13,14] and the Swiss museums of the Baur Foundation and the Ariana museum [15,16] as well as with sets of Chinese and Vietnamese ceramics from previous dynasties (Ming and Yuan) [17–19]. Such a set of exceptional Qing artifacts has never been analyzed or discussed hitherto. Except for a recent study on imperial teapots [20], previous XRF studies are related to shards [21–25], and more common pieces [26–29]. The number of pieces considered is around 60 for Qing objects, and several dozen for objects from Europe (see reference [30] and references herein) or from earlier Chinese (and Vietnamese) periods [17–19]. A few comparable shards have also been analyzed in depth at the laboratory using many techniques [31–33].

The questions we will try to answer concern the identification of the use of raw materials and/or European recipes in the objects and the evolution of technologies during the 18th and 19th centuries. The choice of elements analyzed, and their correlation, will be made on the basis of previous work and information provided by historical documents. We will compare the productions of the imperial workshops (Beijing and Jingdezhen) with those of a private one located in Canton (Gangzhou) used for the Emperor, the Chinese market and for export (*porcelaines de commande*/armorial export porcelain) [31], by defining the similarities and differences between these ‘China-made’ enamels on porcelain and on metal on one hand, and on the other hand, by comparing them with similar productions made simultaneously in Europe.

## 2. Historical Context

As in Japan at the end of the 16th century at the Court of the Nabeshima clan in Arita (Kyushu, Japan, beginning of the Edo period (1603–1868)) [34], the European missionaries (chiefly Jesuits) residing in the different imperial and princely residence (close to the Forbidden City) of Beijing during the reign of the Emperor Kangxi (1662–1722) and his successors Yongzheng (1723–1735) and Qianlong (1736–1795) played a decisive role in the transfer of European enameling and painting know-how to Asian craftsmen. Chinese archives (Qing Palace) and Jesuit correspondence bear witness to the demands of the emperors, to the difficulties and successes in setting up enameling (1693) and glass production (1696) workshops in the imperial workshop at the French church (Beitang), to the arrival of European experts, Jesuits or not (1698 and after), and to the importation of ingredients to obtain a palette of colors, opaque and mixable (1715–1722) allowing the realization of sophisticated realistic enamel decorations rivaling oil painting [35–47]. Such enamel decorations have been made in France since the middle of the 17th century on metalware [48]. The Chinese documents also testify to the numerous exchanges of information but also of craftsmen. This was indeed the case between the imperial workshops of the capital and the imperial kilns of Jingdezhen where the porcelain ‘supports’ were produced, but also with the other, ‘private’ or official kilns of Jingdezhen and the enameling workshops, on porcelain or on metal, of Canton (Gangzhou) [44–47,49].

Let us recall that the production of porcelain in Europe, except the very particular case of the hybrid porcelain of Medici (1575–1587) [50], dates back to ~1670 for the synthesis of soft-paste porcelain (in a way resembling a fritware inspired by ceramics from ‘Iznik’) in Rouen, then Saint-Cloud in France, and Fulham in the United Kingdom [30] and ~1710 for the ‘true’ china, i.e., a mullite-based hard-paste porcelain, in Meissen (Saxony) [51], the latter being very close to Chinese productions because it used similar rocks for the paste (kaolin and kaolin-like rocks, pegmatite, quartz, etc.) [52–55]. The enamels of soft-paste porcelain, with a lead-based flux therefore fired at low temperature (muffle kiln, ~700 to 1000 °C), are heirs to the know-how of majolica enamels, Limoges enamels (metalware) and enamels on glass which allowed a wide palette of colors [1–3,56–59]. On the contrary, hard-paste porcelain glazes fired at a much higher temperature (~1300 °C in China, ~1400 °C in Europe) only offer a reduced palette, rather similar to that of stained glass [1,56]. Indeed, the realization of enamels imposes on this layer of thin glass deposited on an often opaque and non-porous substrate, particular constraints: its low thickness, a few tens to hundred(s) of microns, imposes a significant concentration in coloring agent(s) and a ‘white’ phase, wherein the opacifier usually needs to be added to ‘brighten’ the color [1,2,4,8,56]. The realization of the decoration on a non-porous support (and not on an unfired (green body) or biscuit (porous) paste (first firing around 950 °C)) such as glass, metal or fired porcelain requires the use of media, in particular essences, oils, glues, resins, and not water as for the porous substrate. In the end, the colored areas must be preserved during firing (no interdiffusion or ‘burrs’), and present after firing the shine and the desired thickness without defects (flaking, cracking), which determines the constraints of viscosity, thermal expansion, melting temperature, etc. [2,4,9]. The objects with sophisticated decorations made for the Emperors of China are among the most appreciated ceramic masterpieces, particularly in Asia, and their value rivals that of many paintings by Western great masters. Additionally, no sampling is possible and even transport to a laboratory is rarely possible given the costs of packaging and insurance. The analysis must often be done in the secure place of storage or exhibition. Our previous works [10–16,30,48] have shown that the combination of mobile X-ray fluorescence (pXRF) instruments (information on the chemical elements present) and a mobile Raman microspectroscopy set-up (information on the ‘molecular’ structure, i.e., on the crystalline phases or amorphous) identified the coloring agents and phases present in the glazes and enamels, thus making it possible to compare the raw materials and techniques that were used for preparing, laying and firing the decorations, despite the impossibility of observing the stratigraphy as it is possible on a fracture or a shard [24,25,29,31–34]. However, for a perfect interpretation of the results, the study by the same instruments and other more powerful ones (in particular SEM-EDS, XRD, PIXE and PIGE) in the laboratory of similar shards is essential.

### 3. Materials and Methods

#### 3.1. Artifacts

The analyzed objects are shown in Figure 1, and Table 1 summarizes their information. The pieces were selected to represent the period when technical innovations could be linked to the presence of the European missionaries [10,36–38,45,46,59]. We added to the corpus 19th century porcelains which may have been made after 1850, i.e., using as coloring agents chemically purified raw materials and not ‘simple’ minerals empirically selected and partially transformed by roasting and/or acid attack [6,59]. For comparison, some Canton metalware and Yixing red stoneware previously analyzed were also included [10,15,16].



**Figure 1.** View of analyzed artifacts. Existing marks are presented. The allocated production period is specified (see Table 1 for details).



**Table 1.** Studied corpus (c.: century; ca: circa).























Inventory Number	Description	Remarks	Date	Type (Expected Kiln)	Refs.
Guimet Museum					
G5687 	porcelain		Middle-latter half 17th c.	<i>doucai</i> (Jingdezhen) Private kiln	
G5696 	porcelain	Kangxi mark	Middle-latter Half 17th c.	<i>doucai</i> (Jingdezhen)	[10]
G3361 	porcelain	Kangxi mark	End of Kangxi reign ca 1722	<i>Famille rose</i> (Jingdezhen imperial factory)	[10]
G5250 	porcelain	Kangxi mark	End of Kangxi reign 1715–22	<i>falangcai</i> (Imperial Palace workshop)	[10]
G823 	porcelain	Kangxi mark	<1713	(Imperial factory; Jingdezhen)	
G913 	porcelain	Yongzheng mark	Yongzheng reign 1723–35	<i>yangcai</i> (imperial factory, Jingdezhen)	[10]
G4806 	porcelain	Yongzheng mark	1723–35	<i>yangcai</i> (imperial factory, Jingdezhen)	[10]
MG3668 	stoneware		2nd half 18th c.	Yixing (private kiln)	[10]
G2890 	porcelain	Qianlong mark	Latter half 18th c	(Imperial factory; Jingdezhen)	
MG8062 	stoneware	Qianlong mark	19th c.	Yixing (private kiln)	[10]
G5615 	porcelain		19th c.	(Imperial factory; Jingdezhen)	
G4939 	porcelain		19th c.	(Imperial factory; Jingdezhen)	
MG907 	porcelain		19th c.	Private kiln?	
G2789 	porcelain	Yongzheng mark	19th c.	(Imperial factory; Jingdezhen)?	

Table 1. Cont.

Inventory Number	Description	Remarks	Date	Type (Expected Kiln)	Refs.
Louvre Museum					
R1041	 porcelain	Similar cup at different museums	ca 1720-40	Private workshop (Jingdezhen)	[13]
R1175	 porcelain	English family coat of arms	ca 1735	Private workshop (Jingdezhen-Canton)	[13]
R1177	 porcelain		ca 1735	Private workshop (Jingdezhen-Canton)	[13]
R1045	 porcelain	Similar cup at Rijksmuseum	1730-45	Private workshop (Jingdezhen-Canton)	[13]
TH487	 porcelain		1730-40	Private workshop (Jingdezhen)	[13]
R1048	 porcelain		1740-60	Private workshop (Jingdezhen-Canton)	[13]
R958	 metalware		1730-96	Private workshop (Canton)	[11]
R975	 metalware		1730-96	Private workshop	[11]

Fourteen pieces from the Musée national des arts asiatiques-Guimet and eight from the Département des objets d'art du Musée du Louvre were selected. The selection of objects was guided both by the colour ranges (background and painted decoration) and by the painting techniques. The techniques known as *wucaï* (five colours), *yangcai* (foreign colours) and *falangcai* (foreign colours produced at Beijing imperial workshop) are all represented. The selection also takes into account the plurality of production sites between the capital, Jingdezhen and Canton. The objects in the Louvre come from two important collections built up in the 19th–20th centuries, the collection of President Alphonse Thiers (1797–1877) and that of Salomon de Rothschild (1835–1864). They all belong to the category of so-called *porcelaine d'exportation*. The majority of Guimet's objects are of imperial production. All analysed objects are in porcelain and metal body, as there are no objects in painted enamel in glass body in the collections of these two museums. The chronological frame of the objects included in the analyses is rather broad, ranging from the second half of the 17th century to the 19th century, with the majority of objects produced in imperial workshops or factories during the 18th century.

Pieces with imperial marks offer precise chronological markings, particularly those from the late Kangxi reign (c. 1700–1722, or 1715–1722) and the Yongzheng reign (1723–1735).

More specifically, the G 823 dish, produced on the occasion of Kangxi's 60th birthday in 1713, therefore dates obviously previous to this very year. It provides an important chronological marker for observing the characteristics of imperial production in Jingdezhen during the years of 1710–1730 [60,61]. Among the bowls with imperial mark, several pieces can be compared to items kept currently in the Palace Museum in Beijing and Taipei. G 913 is similar, in the term of the background, the colour palette, of the floral composition, to two bowls (the Guci 11367 and Guci 8663) in the Taipei Palace Museum, both of which are classified as *yancai* colours [60,61]. Their production date corresponds well to the reign mark. However, some of them pose a dating problem. For example, the bowl G 2789 with painted decoration on a black background bears a Yongzheng reign mark raises question of an authentic Yongzheng period production. Analyses are expected to provide elements to better date the production.

An overview of Qing Dynasty enamelware productions can be found in references [60–66]. The rare shards of imperial ceramics analyzed [23,24,32] show glaze thicknesses varying between 20 and 150  $\mu\text{m}$  with a highly heterogeneous distribution both in depth and in the XY color plane. In two close spots of the order of a  $\mu\text{m}^2$ , the quantity of pigment can be entirely different to achieve, for example, different shades of green [14,67].

### 3.2. Method

The procedure has been described in previous articles in detail [12–16,30]. X-ray fluorescence analysis was performed on site using a portable ELIO instrument. The set-up included a miniature X-ray tube system with a Rh anode, a  $\sim 1\text{ mm}^2$  collimator and a large-area Silicon Drift Detector with an energy resolution of  $<140\text{ eV}$  for Mn K $\alpha$ , an energy range of detection from 1.3 keV (in air) to 43 keV. Within the resolution of the pXRF instrument, the Fe K $\beta$  peak and the Co K $\alpha$  peak corresponding to the blue color are located in the same energy range and fitting is required to extract the relative contribution of each. This same procedure is performed to detect arsenic since the position of the As K $\alpha$  peak is in the same energy range as the Pb L $\alpha$  one; lead being present in sufficient quantity in the analyzed enamels that its peaks dominate the recorded EDS spectra (Figures 2–4). The working distance is 1.4 cm. We measured the Diorite D-RN geostandard from the ANRT (*Association Nationale de la Recherche Technique*) in the form of polished rock piece as usual to control the performances of the instrument. Depending on the object, the measurement was carried out by positioning the instrument on the top or on the side. Perfect perpendicularity to the area measured is necessary. Measurements were carried out in the point mode with an acquisition time of 150 s, using a tube voltage of 50 kV and a current of 80  $\mu\text{A}$ . No filter was used between the X-ray tube and the sample. The analysis depth during the measurement of the enamel was estimated from the Beer–Lambert law (analysis depth, defined as the thickness of the top layer from which comes 90% of the fluorescence) [68] to be close to 6  $\mu\text{m}$  at Si K $\alpha$ , 170  $\mu\text{m}$  at Cu K $\alpha$ , 300  $\mu\text{m}$  at Au L $\alpha$ , and 3 mm at Sn K $\alpha$ .

The data fitting procedure has been already used in previous papers [15,16]. After recording the raw data with ELIO, the spectra files were opened in the Artax 7.4.0.0 (Bruker, AXS GmbH, Karlsruhe, Germany) software. For the data treatment process, the studied objects were considered as infinitely thick samples. Before evaluating the analysis data, all of the spectra were imported, and a new method file was created via “Method Editor” of Artax for an applied voltage of 50 kV and current of 80  $\mu\text{A}$ . The corresponding major (e.g., K, Ca), minor (e.g., Fe, Ti, Co, As), and trace elements (e.g., Ag, Bi, etc.) were added to the Periodic Table. For the correction, escape and background options were selected in the Method Editor, and 10 cycles of iteration were selected, starting from 0.5 keV to 45 keV. The deconvolution method, Bayes, was applied to export the data table. The net area was calculated under the peak at the characteristic energy of each element selected in the periodic table, and the counts of the major, minor, and trace elements were determined in the colored areas (white, red, yellow, orange, blue, green, and black). Before plotting the scatter diagrams, the net areas of each element were normalized by the number of XRF photons derived from the elastic peak of the X-ray tube of rhodium. Normalization

with respect to the signal of Si or Co was made for the comparison of certain elements, in particular for the data coming from different measurement campaigns and for artefacts prepared with very different technology at different times (e.g., comparison with Yuan and Ming Dynasty monochrome or blue-and-white porcelain). Then, these normalized data were plotted in the ternary scattering plots drawn for the interpretation and discussion of the results with the software Statistica 13.5.0.17 (TIBCO Software Inc., Palo Alto, CA, USA).

The choice of representing our results with ternary diagrams results in the fact that they allow us to compare, by associations of elements, certain characteristics of the enamels such as their silicate matrix and their colorants used by the craftsmen. The interest in visualizing the distribution of data in ternary diagrams is twofold. Firstly, it allows us to observe potential clusters of points and thus to associate one or more samples with each other. Secondly, these clusters, depending on their distribution within a ternary diagram, can be associated with a type of composition, a recipe/technique, or even a source depending on the elements being compared. For example, the Pb-Ca-K ternary diagram combines the major fluxes analyzed by pXRF and will thus allow us to define the different types of silicate matrices used in the enamels. In addition, the determination of a concentration %wt (which can be done by the ARTAX software) does not make sense because the enamel decoration is very heterogeneous (superposition of layers of variable thickness between a few tens and hundreds of  $\mu\text{m}$  containing variable distributions of pigments and coloring agent). This problem has been discussed in previous works [15,16,69] and the repeatability measurements on reference shards showed that the variability was primarily a function of the intrinsic multi-scale heterogeneity (from micron to cm) of the painted decorations [70].

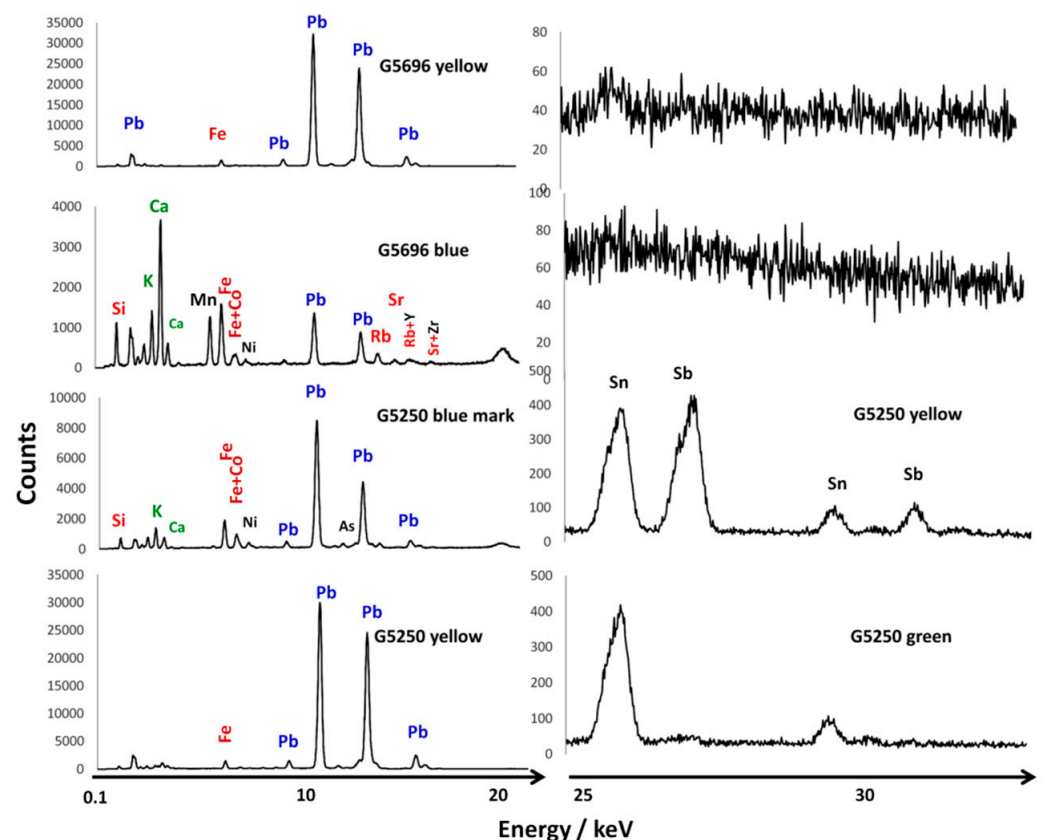


Figure 2. Representative XRF spectra of enameled porcelain (see Table 1 for details).



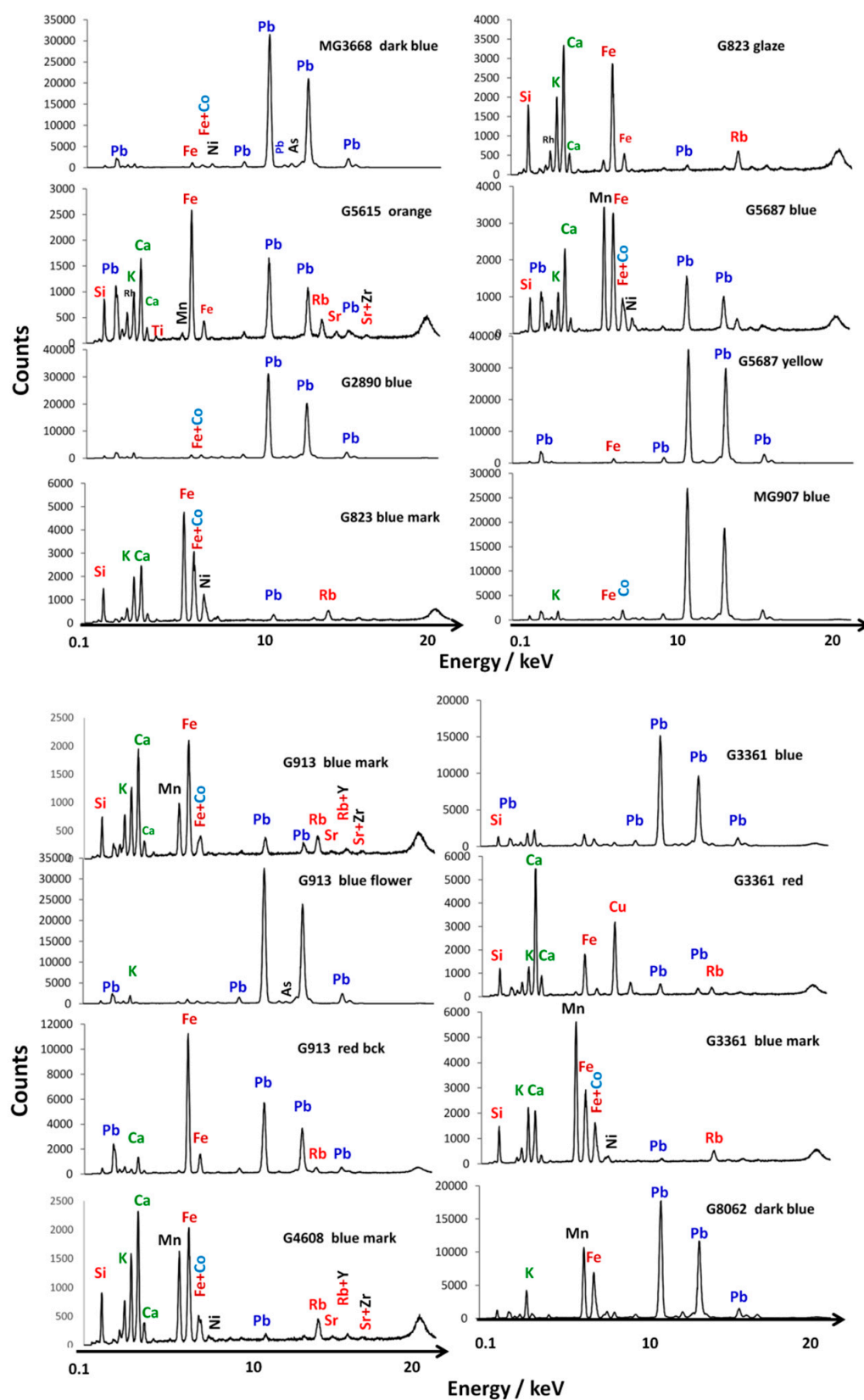
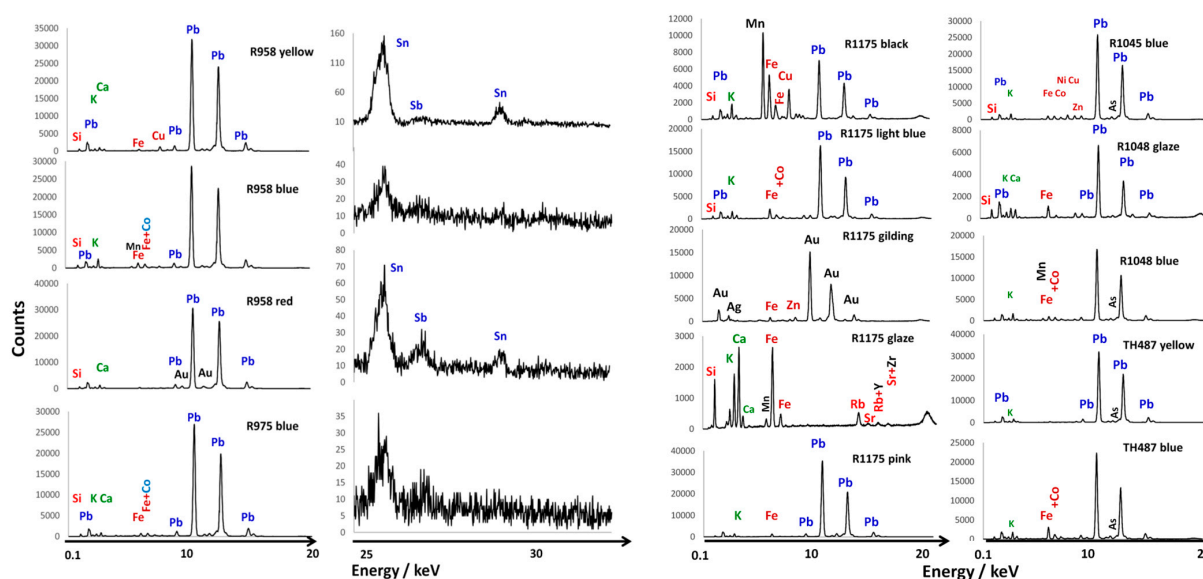


Figure 3. Representative XRF spectra of enameled porcelain (see Table 1 for details).



**Figure 4.** Representative XRF spectra of enameled porcelain and metalware (see Table 1 for details).

## 4. Results

### 4.1. Information That Can Be Obtained from the XRF Fingerprint

The most representative spectra have been selected to be presented in Figures 2–4, all the results being given in a Table. The full set of XRF data is given in Table S1 (Guimet artifacts) and Table S2 (Louvre artifacts). A first set of information is evident from the observation of the spectra in the characteristic energy ranges of the elements present, namely 0.1 to 20 keV for the main elements (Figures 2–4) and 25–32 keV for the tin, antimony and silver (Figures 2 and 4).

The presence of lead causes the spectra to be dominated by its  $L\alpha$ ,  $L\beta$  and  $L\gamma$  transitions peaks plus other minor contributions (for example the yellow zone of bowl G5696, Figure 2). These peaks remain significant even when the presence of lead results from the pollution of the glaze surface during overglaze firing (G5696 blue, Figure 2).

Figure 2 highlights the three technical solutions that were used to obtain colors, ranging from yellow to green: The traditional Chinese recipe with iron ions (bowl *wuca* G5696 yellow) [52], the addition of tin-antimony (bowl *fangcai* G5250, tin yellow and Naples yellow pyrochlore) or the ‘simple’ tin yellow (G5250 green), also easily differentiated by Raman microspectroscopy [1,7,10–16,31,48,56,71–79]. Comparison of the spectrum recorded on the blue decoration of the G5250 *fangcai* bowl with that of the mark of the 5696 *wuca* bowl clearly shows the use of different sources of cobalt, the manganese-rich ‘Asian cobalt’ typical of (late) Yuan productions, Ming productions, and production from the reign of Kangxi before ~1700 [6,80–96] and the ‘European cobalt’ rich in arsenic seen here on the *fangcai* bowl G5250, as has already been highlighted for this object by Raman microscopy [10–12]. An almost identical signature is observed for the *fangcai* bowl G823, and for the Yixing teapot MG3668 (Figure 3) for which the surface pollution of the cover by the overglaze lead is much lower.

On the one hand, for the vase G5687, which is a ‘*Famille verte*’, typical of a production prior to 1700, as expected, we find the use of an ‘Asian cobalt’ rich in manganese. On the other hand, the spectrum of bowl MG907 shows an intense cobalt peak, which is much more intense than that of the associated elements such as iron and manganese. This is characteristic of the use as a source of cobalt from a ‘refined’ chemical product, salts or oxide and therefore of a production after ~1850, in accordance with its attribution on stylistic (visual) criteria of the decoration (19th Century or thereafter).

Figure 4 presents the spectra of metalware R958 and R975 for different colors. Here, tin is detected in all colors due to the need for opacification imposed by the metal substrate.

The red color is obtained by gold nanoparticles (see the small peaks around 10–13 keV on either side of the intense lead peaks), in agreement with the Raman analysis [11].

Generally, the gold signal is difficult to see for the pinks and reds obtained by the gold nanoparticles, as this is the case with the pink color of the R1175 porcelain for instance (Figure 4). However, the gold signature is intense for the golden areas (R1175) and as usual, silver is detected as well, used to improve the gold-ceramic bond [89,91,97–99]. The black color is obtained from a mixture of manganese and copper oxides as usual, that is consistent with the spinel Raman signature [1,4,8]. The other visually detectable elements are the fluxes (potassium and calcium) and their associated impurities (rubidium and strontium); raw material impurities such as yttrium, zirconium and uranium, and other coloring transition metals such as copper, manganese already mentioned, and those associated either with iron (titanium) or with nickel, zinc, etc. and arsenic are also obvious [6]. The main peak of arsenic ( $K\alpha$ ) is superimposed for the resolution of pXRF instruments with the main peak of lead ( $L\alpha$ ), and therefore, only its second peak ( $K\beta$ ) is observable, occurring a little before the second peak of lead [30,48]. Figure 4 shows many examples of this. Iron presents a doublet with an intense  $K\alpha$  peak and a small  $K\beta$  peak attached, about five to six times weaker [30,48]. This last peak is, for the resolution of pXRF instruments, almost confused with the  $K\alpha$  peak of cobalt. Assessing the intensity and width of the peak helps to visually identify the amount of cobalt. To go further in composition comparisons, precise signal processing is necessary. Table 2 summarizes the conclusions that can thus be drawn from the ‘simple’ visual examination of the spectra.

**Table 2.** Comparison between main coloring elements and associated ones, fluxing elements and phases identified by Raman microspectroscopy (The characteristics of the terms underlined or put in italic in the table are explained for each column).

Inventory Number (Expected Date of Production)	Color	Coloring Elements and Associated Elements ( <i>Minor</i> )	Flux (Major, Medium, <i>Minor</i> )	Raman Identified Phase [10,11,13]	Remarks
R1041 (ca 1720–40)	glaze blue yellow pink/rose bck	Fe Co, Fe, Ni, As <u>Fe, Zn, Sn</u> Zn, <u>Au</u>	Ca, K <u>Pb, K</u> Pb, K <u>Pb, K</u>	- - - -	European Co  Au° NPs
R1175 (ca 1735)	glaze black light blue blue pink gilding white	Fe, Mn Mn, Fe, Cu, <u>Co</u> <u>Fe, Co</u> Fe, Co, Ni, As, Cu, Zn <u>Fe, As, Zn</u> <u>Au, Ag, Zn</u> <u>As, Zn, Fe</u>	Ca, K K, Pb <u>Pb, K</u> Pb, K <u>Pb, K</u> Pb <u>Pb, K</u>	Glassy spinel - As-apatite NPs - -	European Co Au° NPs expected
R1177 (ca 1735)	glaze pink/rose yellow + black	Fe, Zn, As, Fe Zn, Sn (Mn, Fe)	K, Ca <u>Pb, K</u> <u>Pb, K</u>	glassy NPs Lead-tin yellow	Au° NPs expected
R1045 (1730–45)	glaze blue bck	Fe <u>Co, Fe, Ni, Cu, Zn, As</u>	<u>K, Ca, Pb</u> <u>Pb, K</u>	Glassy As phase	European Co
TH487 (1730–40)	blue yellow orange red/rose black	Fe, <u>Co, As, Ni</u> Sn, <u>Zn, As</u> Sn, Zn, As, Fe Zn, Fe, <u>As</u> Fe, Mn	Pb, K <u>Pb, K</u> <u>Pb, K</u> <u>Pb, K</u> K, Pb	As phase Glassy + lead-tin yell tr. NPs - -	European Co Au° /Cu° NPs?
R1048 (1740–60)	glaze blue gilding (no gloss) gilding (glossy) yellow red	Fe Mn, Fe, Co, Ni, Zn, As <u>Au, Fe, Ag, Zn, Cu</u> Fe, <u>Au</u> Mn, <u>Sn</u> Fe	Ca, K <u>Pb, K</u> K, Ca <u>K, Ca, Pb</u> <u>Pb, K, Ca</u> Pb, K, Ca	Glassy As-apatite - - Lead-tin yellow Hematite + ?	Eur/Asian Co mixed?

Table 2. Cont.

Inventory Number (Expected Date of Production)	Color	Coloring Elements and Associated Elements (Minor)	Flux (Major, Medium, Minor)	Raman Identified Phase [10,11,13]	Remarks
R958 (1730-96) (metal)	blue yellow red/pink rose/pink yellow-green green gilding turquoise bck	Fe, <u>Co</u> , Cu, As, Mn Cu, As, <u>Zn</u> , <u>Sn</u> <u>Au</u> As, <u>Sn</u> As, <u>Cu</u> , <u>Sn</u> Cu, As <u>Au</u> , Sn, (Sb) Cu, As, Fe, (Sn)	<u>Pb</u> , K <u>Pb</u> , K <u>Pb</u> , K <u>Pb</u> , K <u>Pb</u> , K <u>Pb</u> , K <u>Pb</u> , K <u>Pb</u> , K, Ca	As-apatite As-apatite +lead-tin yell. - As-apatite As-apatite + lead-tin yell. As-apatite - -	Asian + European Co  Au° NPs Au° NPs expected
R975 (1730-96) (metal)	blue yellow white green light green pink/rose black	<u>Co</u> , Fe, As, Ni, (Sn) <u>Zn</u> , <u>Sn</u> , (As) <u>As</u> , Fe, (Ni, Cu) Cu, Zn, As, (Sn) <u>Cu</u> , Zn, Sn, <u>As</u> Fe, As Mn, Fe, Cu	<u>Pb</u> , K <u>Pb</u> , K <u>Pb</u> , K <u>Pb</u> , K <u>Pb</u> , K <u>Pb</u> , K <u>Pb</u> , K	As-apatite As-apatite +lead-tin yellow As-apatite As-apatite As-apatite As-apatite	European Co     Au° NPs ?
G5687 (Middle-latter half 17th c.)	blue yellow red green black paste	Mn, Fe, ( <u>Co</u> ) Fe Fe Cu Cu, <u>Mn</u> , <u>Fe</u> Fe	<u>Ca</u> , K, ( <u>Pb</u> ) <u>Pb</u> <u>Pb</u> , Ca <u>Pb</u> <u>Pb</u> <u>Ca</u> , K, ( <u>Pb</u> )	glassy glassy hematite glassy spinel -	Asian Co
G5696 (Middle-latter half 17th c.)	glaze blue blue mark yellow green red paste	Fe Mn, Fe, ( <u>Co</u> ) Mn, Fe, ( <u>Co</u> ) Fe Cu Fe, ( <u>Cu</u> ) Fe	<u>Ca</u> , K <u>Ca</u> , K, <u>Pb</u> <u>Ca</u> , K <u>Pb</u> <u>Pb</u> <u>Pb</u> , Ca K, Ca	- - - - - - -	Asian Co Asian Co    Cu° NPs ? or hematite
G3361 (ca 1722)	glaze blue blue mark red rose/mauve green yellow-green white	Fe Fe, <u>Co</u> , Cu, As Mn, Fe, <u>Co</u> <u>Cu</u> , Fe Fe, Co, Cu, As Cu Cu, Sn Fe, Cu, <u>As</u>	<u>Ca</u> , K <u>Pb</u> , Ca, K K, Ca <u>Ca</u> , K <u>Pb</u> , K, Ca <u>Pb</u> <u>Pb</u> <u>Pb</u> , Ca	- As-apatite - quartz As-apatite glassy Lead-tin yellow As-apatite	European Co Asian Co, underglaze Cu° NPs ? Cu° or Au° NPs?
G5250 (1715-22)	glaze blue mark dark blue yellow green yellow-green rose/mauve black white	Fe Fe, <u>Co</u> , Ni, As Co, As, Ni Fe, <u>Sn</u> , <u>Sb</u> , <u>Zn</u> Sn, Cu Cu, Fe, <u>Sn</u> Fe, <u>As</u> , <u>Au</u> Fe <u>As</u> , Fe	K, Ca <u>Pb</u> , K, Ca <u>Pb</u> , K <u>Pb</u> , Ca <u>Pb</u> , K <u>Pb</u> <u>Pb</u> , K, Ca <u>Pb</u> , Ca <u>Pb</u> , K	- - As phase Sb pyrochlore - Lead-tin yellow NPs signature - -	European Co overglaze Co peak too strong?    Au° NPs
G913 (1723-35)	glaze blue mark blue flower red background white yellow green black paste	Fe Fe, Mn, ( <u>Co</u> ) Fe, <u>Co</u> , Mn, Ni, Cu, As Fe Fe, Mn, <u>As</u> , Co Fe Cu, (Sn, Sb) <u>Mn</u> , Fe, Ni, Cu Fe	Ca, K <u>Ca</u> , K <u>Pb</u> , K Ca, Pb <u>Pb</u> , K <u>Pb</u> <u>Pb</u> <u>Pb</u> K, Ca (Pb)	- - - Hematite - Glassy + lead-tin yell. Tr. Glassy Spinel -	Asian Co underglaze Eur/Asian Co mixed ?



Table 2. Cont.

Inventory Number (Expected Date of Production)	Color	Coloring Elements and Associated Elements ( <i>Minor</i> )	Flux (Major, Medium, <i>Minor</i> )	Raman Identified Phase [10,11,13]	Remarks
G4806 (1723-35)	glaze blue mark blue yellow green white rose	Fe Mn, Fe, ( <u>Co</u> ) Fe, ( <u>Co</u> , <u>Cu</u> , <u>As</u> ) <u>Fe</u> <u>Cu</u> <u>Fe</u> <i>Mn, Fe</i>	<u>Ca</u> , <u>K</u> <u>Ca</u> , <u>K</u> <u>Pb</u> , <u>K</u> <u>Pb</u> <u>Pb</u> <u>Pb</u> <u>Pb</u>	- - Glassy Glassy + lead-tin yell. tr.? - hematite	Asian Co underglaze European Co     +Au° NPs ?
MG3668 (2nd half 18th c.)	dark blue yellow rose/pink white black turquoise yellow-green	Fe, Ni, <u>Co</u> , As Fe, <u>Sn</u> As, Fe, Zn <u>As</u> , Fe <u>Cu</u> <u>Cu</u> , <u>As</u> , <u>Sn</u> , <u>Fe</u> <u>Cu</u> , <u>Sn</u> , <u>As</u> , <u>Fe</u>	<u>Pb</u> , <u>K</u> <u>Pb</u> , <u>Ca</u> <u>Pb</u> <u>Pb</u> <u>Pb</u> <u>Pb</u> <u>Pb</u>	As-apatite Lead-tin yellow NPs - Spinel - As-apatite + lead-tin yell.	European Co  Au° NPs
G823 (18th c. <1713)	glaze blue mark dark red orange dark green	Fe Mn, Fe, ( <u>Co</u> ) <u>Fe</u> <u>Fe</u> <u>Cu</u>	<u>Ca</u> , <u>K</u> <u>Ca</u> , <u>K</u> <u>Pb</u> , <u>Ca</u> <u>Ca</u> , <u>Pb</u> , <u>K</u> <u>Pb</u>	- - hematite hematite glassy	Asian Co underglaze
MG8062 (19th c. ?)	dark blue light blue brown bck	Fe, <u>Co</u> , As, ( <u>Cu</u> ) Fe, <u>Co</u> , As <u>Fe</u> , <u>Ti</u>	<u>Pb</u> , <u>K</u> <u>Pb</u> , <u>K</u> <u>K</u>	As phase As-apatite -	Eur. Co: <1850! Eur. Co: <1850!
G5615 (19th c.)	glaze green orange yellow black	Fe <u>Cu</u> <u>Fe</u> Fe, <u>Sn</u> , <u>Cu</u> <u>Cu</u> , <u>Mn</u> , <u>Fe</u>	<u>Ca</u> , <u>K</u> , <u>Pb</u> <u>Pb</u> <u>Ca</u> , <u>K</u> , <u>Pb</u> <u>Pb</u> <u>Pb</u>	- - - - -	
G4939 (19th c.)	glaze rose bck blue mark	Fe Fe, <u>Au</u> , Zn Mn, Fe, <u>Co</u>	<u>K</u> , <u>Ca</u> <u>Pb</u> , <u>K</u> <u>K</u> , <u>Ca</u>	- - -	Au° NPs Asian Co underglaze
MG907 (19th c.)	blue dark blue blue mark white yellow green gilding red paste	<u>Co</u> , As <u>Co</u> , Fe, <u>Cu</u> , As, Ni Fe, Mn, ( <u>Co</u> ) <u>As</u> , <u>Cu</u> , Fe, <u>Sn</u> <u>Sn</u> , Fe, <u>Cu</u> <u>Cu</u> , <u>Co</u> , Fe, As, <u>Sn</u> <u>Au</u> , Ag, Fe, <u>Cu</u> <u>Fe</u> Fe	<u>Pb</u> , <u>K</u> <u>Pb</u> , <u>K</u> <u>Ca</u> , <u>K</u> <u>Pb</u> <u>Pb</u> <u>Pb</u> , <u>K</u> <u>K</u> , <u>Ca</u> <u>Ca</u> , <u>K</u> , <u>Pb</u> <u>K</u> , <u>Ca</u>	- - - - - - - - -	Co purity >1850 Co purity >1850 Asian Co underglaze
G2789 (19th c.)	glaze red mark black green light green white 'gilding' gilding paste	Fe <u>Fe</u> <u>Cu</u> <u>Cu</u> <u>Cu</u> , <u>Sn</u> , As, Fe <u>As</u> , <u>Cu</u> , Fe <u>Cu</u> <u>Cu</u> , Fe, <u>Au</u> Fe	<u>K</u> , <u>Ca</u> <u>K</u> <u>Pb</u> <u>Pb</u> <u>Pb</u> <u>Pb</u> <u>Pb</u> <u>Pb</u> , <u>K</u> , <u>Ca</u> <u>K</u>	- - - - - - - - -	False gilding True Au° gilding

Table 2. Cont.

Inventory Number (Expected Date of Production)	Color	Coloring Elements and Associated Elements (Minor)	Flux (Major, Medium, Minor)	Raman Identified Phase [10,11,13]	Remarks
G2890 (Latter half 18th c)	blue	Fe, <u>Co</u> , Cu, Ni, Zn, As	<u>Pb</u> , K	-	Eur. Co >before 19th c.
	dark mark	Fe	K, Ca	-	
	yellow	Sn, Fe, Zn	<u>Pb</u> , K	-	Au <sup>o</sup> NPs
	rose	Fe, Sn, <u>Au</u> , Zn, Cu	<u>Pb</u> , K	-	
	green	<u>Cu</u> , Fe, <u>Sn</u>	<u>Pb</u> , K	-	
	orange	Mn, Fe, <u>Sn</u>	<u>Pb</u> , K	-	
	black	Mn, Fe, <u>Cu</u>	<u>Pb</u> , K	-	
	paste	Fe	K, Ca	-	

Eur.: European; tr.: traces; -: not studied; NPs: nanoparticles.

As already observed in the study of the Baur Foundation bowls with the imperial mark [15,16], the cobalt used for the underglazed marks is rich in Mn, which is in agreement with an application of the mark on the porcelain green paste in Jingdezhen kiln with a cobalt from Asian sites. On the contrary, the blue areas of the decorations use cobalt of complex composition (As, Ni, Cu) in accordance with an imported material and the enamel is lead-based. The *wuca* G5687 and G5696 pieces, the oldest in our selection, use Asian cobalt for the decoration. As concluded from the Raman analysis, the G3361 pot appears to be one of the first objects using imported materials. G2890 bowl expected from 19th century is made with impure European cobalt that is consistent with a production before the development of cobalt refining, i.e., before ~1850. False copper-based gilding in combination with true Au<sup>o</sup> gilding is identified for the G2789 bowl. Such a technique was already identified in 18th century Meissen ‘gilded’ *boccaro* ‘porcelain’ [99].

For a clear identification of the use of Cu<sup>o</sup> or Au<sup>o</sup> NPs for the production of a red to violet/mauve color combination of the Raman and XRF techniques is required due to the low amount of metal NPs required and hence its difficulty to detect by XRF. Combination of a ‘simple’ Raman signature of the glassy coating with the identification of the Fe element attests to the use of iron ions (Fe<sup>3+</sup>) to obtain the yellow color (e.g., G4826, G5687 and G5696). Traces of lead-tin are detected by Raman microspectrometry (e.g., G913 and G4806).

#### 4.2. Towards a Semi-Quantitative Comparison

We underlined in the experimental part the problem of the variability of the depth probed by the X-ray photons according to their energy [68,69], penetration depth being able to be much lower (light elements) or much higher (heavy elements) than the thickness of the layer of colored enamel [69]. Only for the transition metals are the characteristic peaks located in an energy range inducing a penetration of the same order of magnitude as the standard painted enamel layer (100–200 µm) [10,31]. In addition, by nature, a painted enamel decoration is heterogeneous in a chromophore in the three directions of the colored layer and this for lower scales or of the order of magnitude of visual acuity (a few microns) [67]. Unlike ‘solid’ glass objects (crockery, stained glass) or thick ‘monochrome’ enamel layers—a layer of celadon enamel can exceed several millimeters [19,59]—the concept of composition therefore makes no sense for painted enamels and we have proposed a particular procedure for comparing enameling techniques, the comparison of the localization of the characteristic signals of the different chemical elements (after correction of the continuous background as possible for example with the Artax data processing software) in ternary diagrams relevant to the raw material composition and ceramic process [15,16]. Clustering data should correspond to rather similar element content in the analyzed volume.

#### 4.3. Comparison of Silicate Matrices

An enamel is a totally amorphous glass, whether containing chromophore ions, bubbles or a formation of several amorphous phases, or else a glass-ceramic, i.e., a composite

material containing a dispersion of phases introduced before firing into the precursor powder (which is a pigment containing one or more chromophores or opacifier characterized by a higher optical index than that of the silicate matrix; these phases must be very chemically stable so as not to be attacked, dissolved by the enamel in fusion during firing), or forming on cooling from the saturation of certain elements of the molten enamel. We will first consider the ternary diagrams regarding elements having the role of a flux, that is to say lowering the melting point, controlling the viscosity, etc.; these comprise potassium, calcium, lead and arsenic (the present analytical method cannot detect boron, lithium and sodium), these elements being able to have other specific effects on thermal expansion, chemical resistance, opacification, etc. [2–4,8,9]. The natural impurities of these elements, namely rubidium and strontium will also be considered (Figure 5).

The Ca-Rb-Sr ternary diagram (Figure 5) constructed from ‘blue’ enamels highlights 3 or 4 clusters: Two large groups, one parallel to the Ca-Rb side and the other enriched in strontium; MG8062 (19th c.) forms an intermediate cluster like the *falangcai* bowl blue G5250. We therefore have 3 types (origins) of raw materials (which we will call RMCa, RMSr and RMInt). The same classification is possible for enamels of other colors. The pastes are located in the RMCa cluster, which leads us to associate this group with the use of raw materials from Jingdezhen, where the workshops which produced the vast majority of the studied objects were located. From the Ca-Rb-Sr ternary diagram, it is clear that the white enamel of artifact G5250 is quite heterogeneous but rather similar to that of the G8062 blue analogue. A third group or a mixture of the other two groups explains the location of the enamels of the Yixing bowl MG8062 and the *falangcai* bowl G5250. The Pb-Ca-K and Pb-Cu-As ternary diagrams provide additional information.

We will first discuss the objects of the mnaa-Guimet Collection (Figure 1, Table 1). The Pb-Ca-K ternary diagram separates the enamels in which lead constitutes the main flux (all located towards the Pb top summit) from the enamels (and paste) whose surface has been polluted by the lead evaporating during the firing of the overglaze (PbO is very volatile above 850 °C). Potassium-rich pastes (located on the Pb-K side) are also separated from most calcium-rich glazes. The Pb-Cu-As diagram highlights 3 special cases: the black background of bowl G2789 is rich in copper (known to be a well-established technique [1,4,8,98,99]); the pink/rose of the G5250 bowl is enriched with arsenic and, as the Raman analysis indicates the use of metallic nanoparticles, coloring by gold nanoparticles is expected; the red color of the rose in the G3361 pot is obtained with Cu<sup>0</sup> nanoparticles (which is in agreement with the Raman analysis which indicates that the red color is not obtained as conventionally by hematite [10]). The use of copper nanoparticles (Cu<sup>0</sup>) is a technique used since the 10th century (Jun ware) by Chinese potters [100–104].

The Y-Rb-Sr ternary diagram classifies the enamels into two groups, a main group and a second on a line defining the same Y/Sr ratio where the pot G3361 and the bowl *falangcai* G5250, the bowl G2789, MG907 and MG3668 are located. The ternary diagram constructed by normalizing the signal of strontium by the signals of rubidium, yttrium and zirconium highlights two aligned groups for defined Y/Zr ratios (colorless glazes are part of this group) and Rb/Zr. We find a relationship between certain enamels and glazes as found for the pastes, which is consistent with the use of the same raw materials, namely those of Jingdezhen.

We find, on the Pb-Ca-K diagram of Figure 6, the same two groups of lead-based enamels and those unpolluted or little polluted during firing, plus an intermediate group for the golden areas (R1175, R1045, R1048 and R1177), which would indicate a mixed matrix with an intermediate lead content and/or the addition of other fluxing agents. The same is true for the Pb-Cu-As diagram where this group is clearly identifiable. It is difficult to know if the distribution towards the Cu at the top is caused by the contribution of the metallic substrate for the artifacts R958 and R975. The two groups identified in Figure 6 for the Sr diagram normalized by Rb, Y and Zr are found and the alignment of the data showing the defined Y/Sr ratio is clear, the golden and white colors being richer in Rb

while the enamels of objects R1045, R1048, R1175, R1177 and TH487 (all of the Yongzheng period) are ‘richer’ in yttrium.

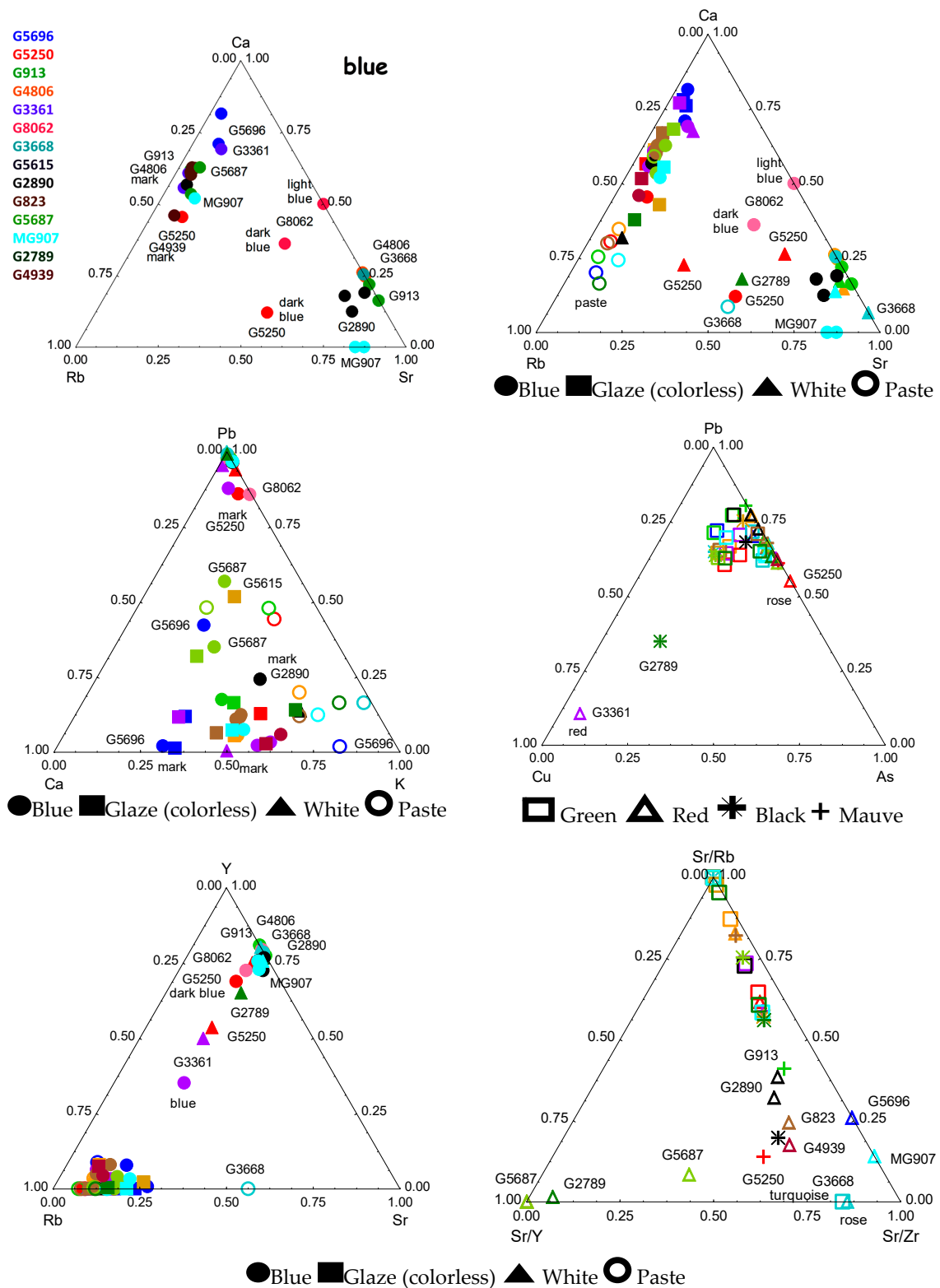


**Figure 5.** Comparison of the signal of flux elements (Pb, Ca, K) of matrices of blue, white or colorless, green, rouge/pink/mauve enamels and pastes and associated elements (Sr, R, Y) (Coll. mnaa-Guimet). The inventory numbers are given; the color of the symbol is that of the enameled area.



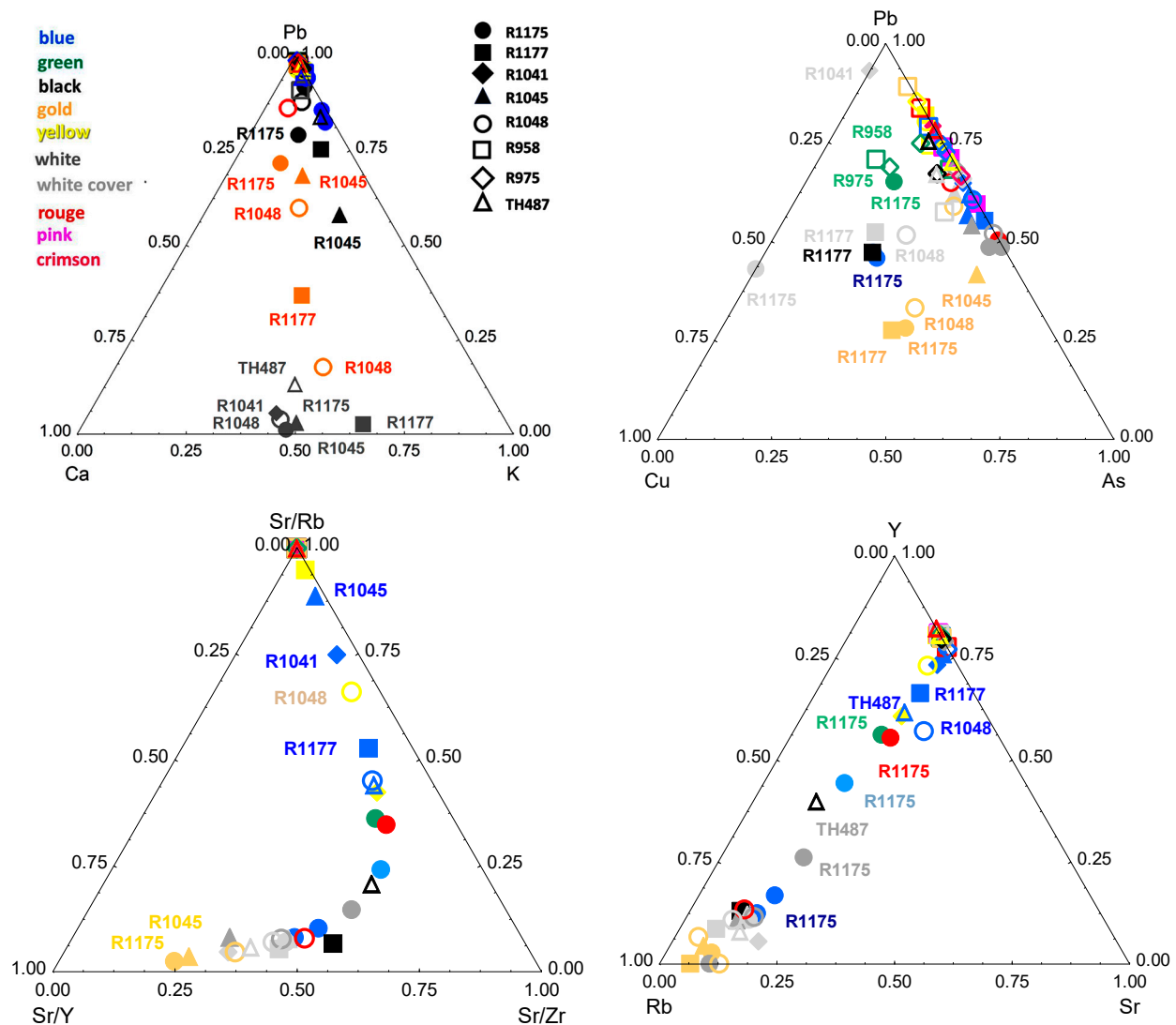


**Figure 6.** Comparison of signal of flux elements (Pb, Ca, K) of enamel matrices and associated elements (Sr, R, Y, As) (Coll. Louvre). See legend to Figure 5 for explanation of symbols.

#### 4.4. Comparison of Coloring Agents

Figure 7 compares the distributions of the signals relating to the color blue, i.e., cobalt and the associated elements, arsenic, manganese and nickel. The use of blue ingredients imported from Europe by European missionaries is well established [35–44,46,47]. One of the main sources of the blue color produced in Europe from the early 16th century is a potassium glass called smalt with about 10 to 20 wt% CoO potassium [6]. Smalt was a by-product of the mining of silver, then of bismuth. Cobalt was specifically mined only at the end of the 17th century [6]. Consequently, the set of associated elements depends both on the ore's composition and its processing.

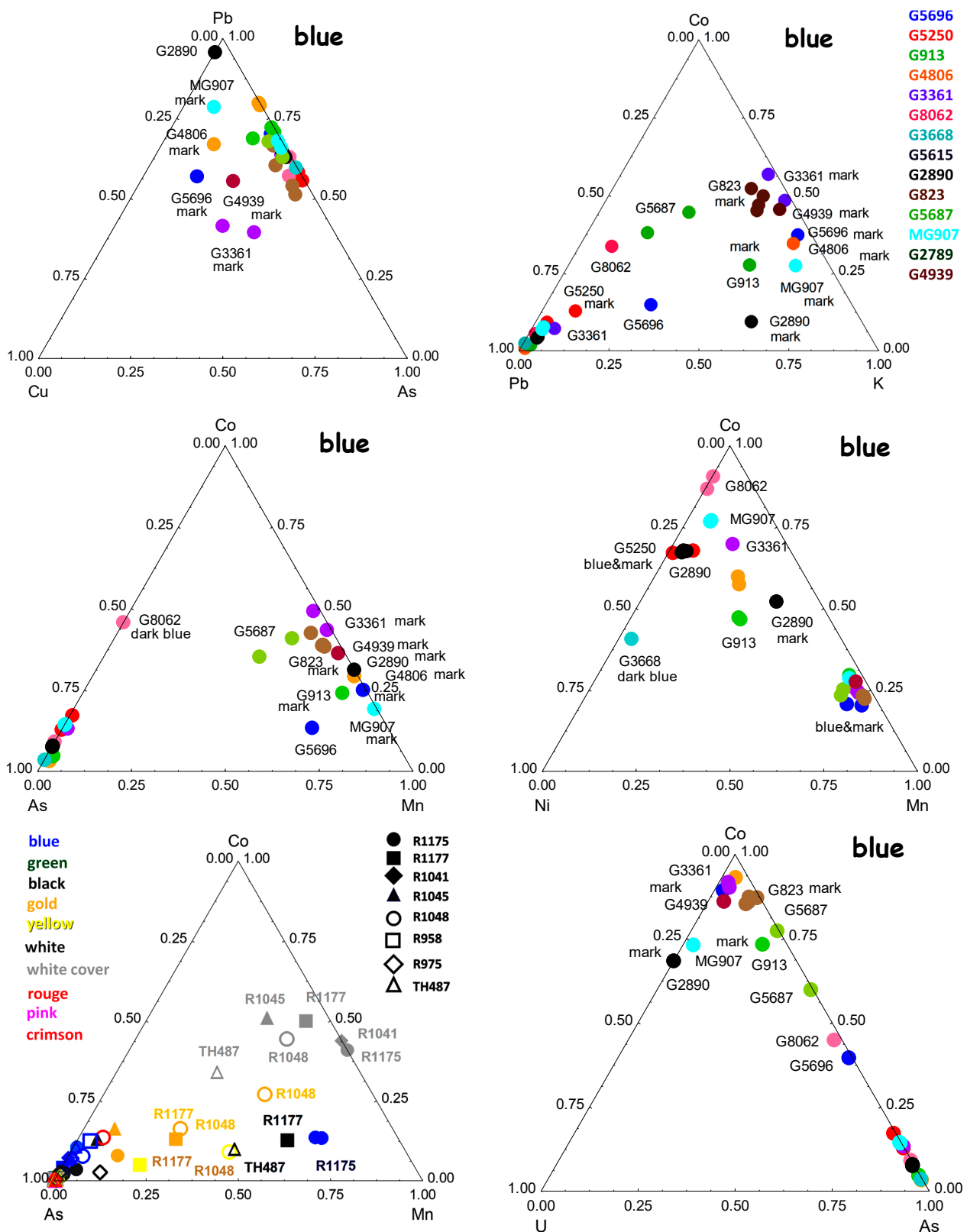


**Figure 7.** Comparison of the signal of elements associated with cobalt (Mn, Ni, U and As) for blue enamels (**top** and **center**, Coll. mnaa-Guimet) and for all enamels (**bottom**, Coll. Musée du Louvre). See legend to Figure 5 for explanation of symbols.

Copper is either an addition to adjust the color or is already present in ancient cobalt sources (17th century and before) [6,30]. On the Co-Pb-K diagram, two clusters can be distinguished, the series of blue marks (G3361, G4939, G5696, G4806, G823, MG907, and G913) corresponding to underglaze marks, of which most of the potassium likely come from the contribution of the glaze above and around the blue lines, the analysis being conducted on the surface with a spot larger than the blue lines. Thanks to the measurements made on different spots on a same object, the variability/error of the measurements can be well illustrated by the distribution of the points. The mark of the G5250 specimen corresponds to a lead overglaze enamel composition. The highest level of copper is observed for the ancient objects, G5606, G3361 and G4806 as previously observed [30]. G2890 appears to be arsenic-free, consistent with its production after 1850, as already noted from other criteria.

The Co-As-Mn diagram differentiates manganese-rich Asian ‘cobalts’ (marks of G3361, G4939, G4806, MG907, G823, and G913; patterns of G5687 and G5696) from possibly arsenic-rich European ‘cobalts’ (patterns of G8062, MG907, G3361, G913, G4939, and G4806) [6]. Iranian cobalt ores also contain arsenic in significant proportions, but the archives explicitly indicate the use of European or Chinese sources. The blue of the decoration of the Yixing G3668 teapot is unusual, which is confirmed by the Co-Ni-Mn diagram. This diagram specifies the differences between the different ‘cobalts’: the richest in manganese are G5687 (decoration), G5696 (decoration and mark), and marks for G823, G3361, G4806, G913, and MG907.

We find that the bowl G8062 is made of ‘pure’ cobalt, so its production will be after 1850. For the artifacts of the Louvre museum (Figure 1, Table 1), only the blue of R1175 is rich in manganese, all the other blues are rich in arsenic and can have thus only been prepared with ingredients imported from Europe. We note the presence of arsenic in the red colored areas (R1045, R1048), of which three hypotheses are possible: firstly, an As-based opacifier has been dispersed in the red precursor powder, or secondly, a background white layer has been deposited. Alternatively, thirdly, the arsenic can be associated with the red chromophore.

Figure 8 compares different diagrams relating to the colors yellow, orange, brown and gold. The Pb-Ca-K diagram highlights the colors where traces of lead are derived only from a pollution product during the firing of other colors: namely, orange G823, orange G5615, golden MG907 and brown G8062; these cases are also distinguished by the presence of copper.

Golden MG907 and G2789 colors have different grades of gold, both containing some copper, with MG907 being the ‘purest’. The Sn-Au-Sb diagram classifies these colors into three groups with tin yellows (G3668, G2890, G5615 and MG907), Naples yellow rich in antimony (G2789, G4806, and G3361) and mixed Naples yellow (G5615, G5687, G913, G5615, and G4806); different glazes can be observed on the same object. In the Pb-Ca-K diagram, the alignment of points along a straight line starting from pole lead with a constant calcium/potassium ratio comes from the variable contribution of the substrate (glaze) due to the variable thicknesses of the overglaze enamels, but less than the depth explored by the incident X-ray beam.

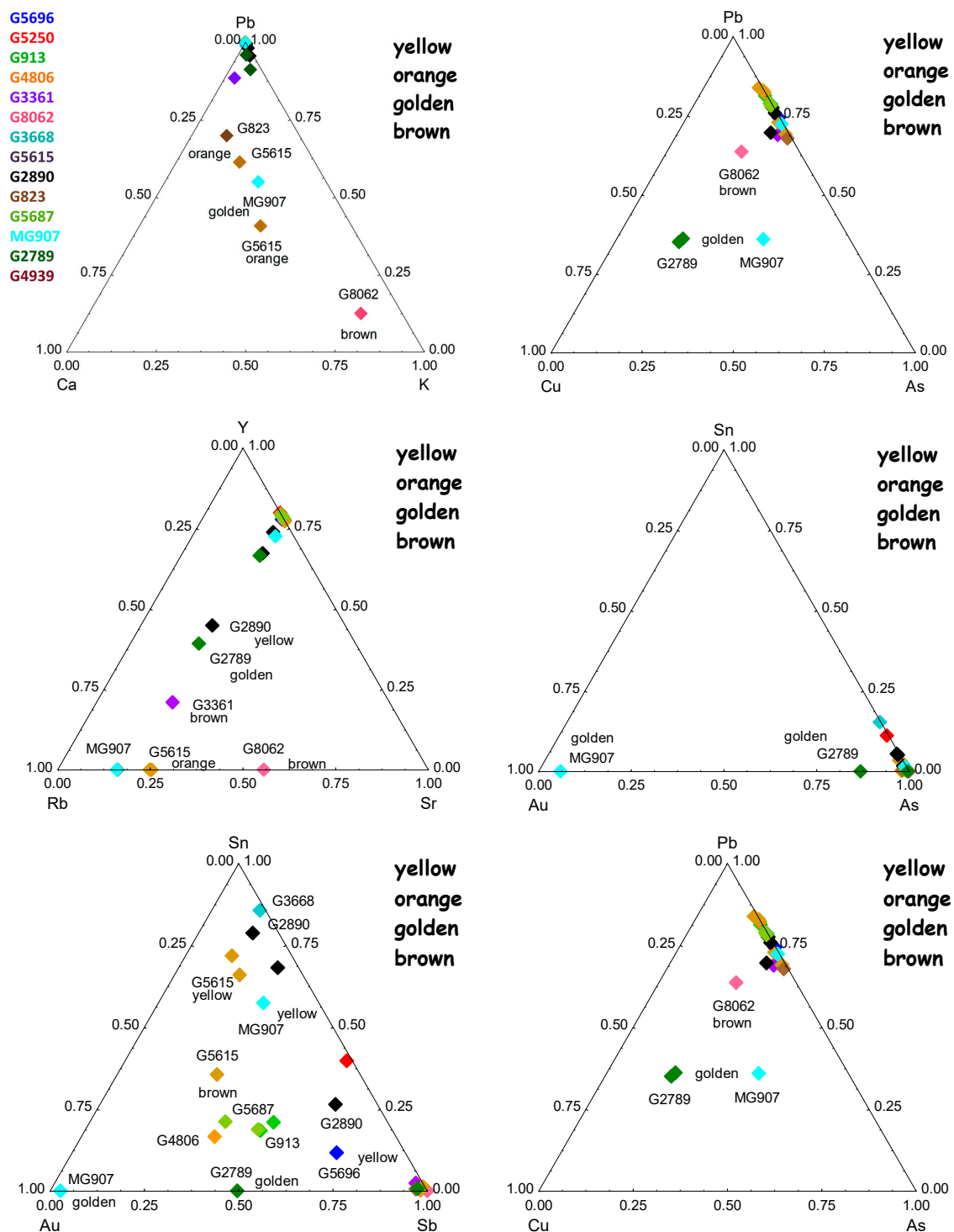


**Figure 8.** Comparison of signal of elements associated with the colors yellow, orange, brown and gold. See legend to Figure 5 for explanation of symbols.

#### 4.5. Red to Pink Color. Gold Nanoparticle Preparation

The comparison of the XRF signals relating to the elements Au, Sn and As for the different colors ranging from pink to violet and mauve (Figure 9), shows that these colors can be obtained by gold or copper nanoparticles, but also by a red pigment such as hematite or hercynite, which will enable us to determine the method of preparation of colloidal gold. Indeed, it is established that, in the 17th century in Europe, two techniques were used for the preparation of colloidal gold from a solution of gold in *aqua regia* (mixture



of nitric and hydrochloric acid): Precipitation by either the addition of tin (a technique known as Kunckel or Cassius' purple) [105,106] or the addition of arsenic (a technique known as Perrot' or ruby glass) [107,108], these two techniques both originating from Italy. By oxidizing, both tin and arsenic can assume several oxidation states, which lead to the reduction of gold ions into metallic nanoparticles.

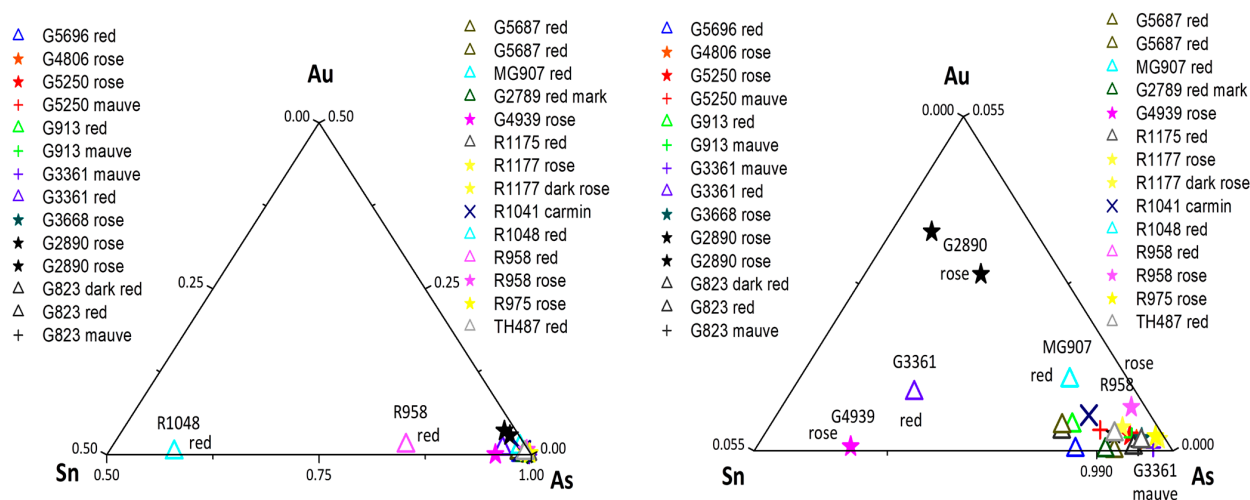


**Figure 9.** Comparison of the signal of elements associated with the use of gold.

The colloidal gold signal is always very weak because the coloring power of the plasmon of the NPs is very high, and a very small quantity of it is sufficient. Zooms were also made near the arsenic pole. We note that only the reds of metalware R958 and (Meissen imitating) porcelain R1048 contain a little tin, and almost no gold (red is obtained with iron oxide hematite, Table 2), and for all the others, tin is found in only trace quantities (Figure 9, left). The maximum zoom (Figure 9, right) shows 2 groups, those where gold is associated with traces of tin (G2890 bowl, pink; G3361 pot, red; G4939 bowl, pink background) and all the others found to be rich in arsenic. Only the colors of the first group can be considered as Cassius purple. For the others, two solutions are possible: Their preparation by the Perrot method and/or the voluntary addition of arsenic as an opacifier. Opacifier is most likely for rose, or carmine and not for red. So, for G5687 17th c. wucai, G5696 17th wucai, G913 Yongzheng bowl, TH487 Yongzheng plate, G823 Qianlong plate, G2789 19th c. bowl, red MG907 bowl 19th c., and R958 Qianlong metal plate specimens, the Perrot' technique is the most likely.

## 5. Discussion: Comparison between Qing Productions and with Ming /Yuan Ones

The objective of this work was to identify in a non-invasive way and at the actual site of conservation of the objects those whose glazes were prepared by recipes or ingredients imported from Europe, as specified in the documents of the imperial archives and in the correspondence of the Jesuit missionaries [36–39,44,46,47,109,110]. The geological contexts of the regions where Chinese potters sourced their supplies during the Yuan, Ming and early Qing Dynasties, i.e., regions marked by the 'recent' Himalayan geological context, differs greatly from that of European sources associated with old (Hercynian) massifs and therefore, the elements associated with cobalt are very different [6]. This is why we will compare with the XRF signals the elements Mn and Fe ('Chinese' context) and Ni and As (European context), as already carried out with objects from the collections of the museums of L'Ariana and the Baur Foundation [15,16]. In these latter studies, we also shown that the major elements and impurities associated with materials used in the first steps of the preparation of the silicate matrix (potassium, calcium, rubidium, strontium and yttrium) have effectively classified the Chinese or European origins of the productions. The diagrams are shown in Figure 10. As, by essence, a painted decoration is made by

varying the cobalt concentration, the XRF characteristic signals of the different elements are normalized with respect to the cobalt signal.

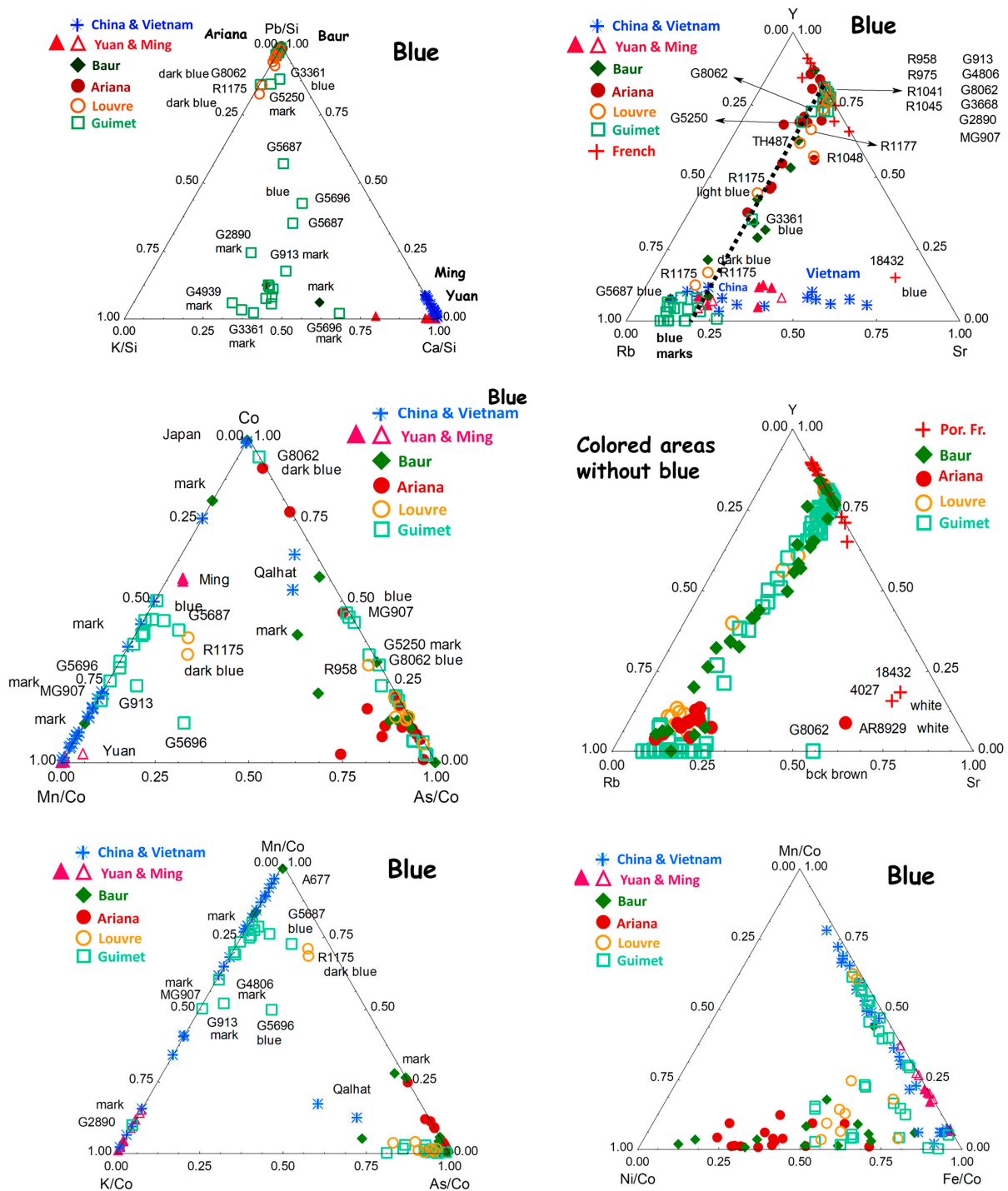


**Figure 10.** Comparison of signal of elements associated with the blue colored areas for artifacts from different origins: Yuan and Ming Dynasty Private Museum Collection [17,18], archaeological shards issued from sites from Ming Dynasty period [19], Baur Foundation Collection [15,16], Ariana Museum Collection [15,16], French porcelain [30] and present study (Louvre and mnaa-Guimet museum Collections). A comparison is made with other colored areas.

Similarly, to compare the impurities of other raw materials, we normalize with respect to the silicon signal, which makes it possible to take into account the variable thickness of the enamel. This last normalization is coarser in the concept.

### 5.1. Enameling Technology

The Pb-K-Ca diagram normalized to the Si signal and the Y-Rb-Sr diagram illustrate that the high temperature underglaze decorations are concentrated towards the Ca/Si apex (Ming and Yuan) and the lead-rich enamels towards the apex Pb/Si (essentially Qing enamels). Added to this is a number of enamels of objects from the mnaa-Guimet collection, roughly aligned along a similar K/Ca ratio. This might indicate glazes prepared with mixed Pb-Ca-K fluxes, glazes of variable thickness, the measurement of lead being made on a high thickness, or the effect of the pollution of the surface of the glazes during the firing of the overglaze explaining why all the underglaze marks appear in the lower part of the diagram. We find a similar configuration for the Y-Rb-Sr diagram. On this diagram, we have also plotted the data for French soft-paste porcelain decorations [30]. The Y-Rb-Sr diagram shows three groups: (i) Enamels/glazes prepared with Chinese raw materials, rich in rubidium (Vietnam productions are enriched in strontium); (ii) those prepared with European raw materials, rich in yttrium and (iii) the intermediate cases explained by the use of a mixture of raw materials. We find the same distributions with the objects from the Ariana and Baur Foundation collections [15,16]. The differences between porcelain of Chinese/Vietnamese (Ming period) and French origins are obvious and the Qing productions are aligned between these extremes, proving the mixture of ‘Chinese’ and imported ingredients. The list of objects in the decoration using mainly European ingredients is listed in the figure. The more the value moves along the line parallel to the Y-Rb side, the more the proportion of Chinese raw materials increases; thus, for underglaze marks, we find that these belong to the ‘Ming’ cluster. The results are similar for the other colors but with more intermediate data, probably due to the varying proportions of the opacifier arranged according to the colors.

### 5.2. Cobalt Sources

The Co-Mn/Co-As/Co diagram classifies objects made with ‘pure’ cobalt from the chemical industry (a 20th c. Japanese porcelain, the bowl MG8062 dating to the 19th c. and the mark reported later from the bowl #616 of the Baur Foundation Collection [15,16]). This also classifies cobalt colors associated with arsenic and those rich in manganese, i.e., made with ‘cobalt’ of Chinese traditions. In the latter, there are the marks affixed at Jingdezhen underglaze. Intermediate data indicate the use of a third type of cobalt (e.g., G5687 and G5696 *wucaï*) or a mixture (R1175). The classification of blue decorations can be done with the Mn/Co-K/Co-As/Co and Mn/Co-Ni/Co-Fe/Co diagrams. We observe the differences between the cobalt of the underglaze marks and that of the overglaze enamels. The comparison with the measurements on the objects of the L’Ariana museum, attributed to the workshops of Canton, shows that the cobalt used in the latter is richer in nickel, therefore this is attributable to a European source [6]. We also find that objects from the mnaa-Guimet use ‘Chinese’ cobalt and mixtures.

Figure 11 compares the signal of the main elements present in the areas colored in yellow, green/turquoise, and brown/orange. The data has been normalized with the source signal to improve the comparison. We see that the orange color is a color of the glaze and not attributable to the lead enamel. The Zn-Sn-Sb and Co-Cu-Sn ternary diagrams show that the green/turquoise colors are always colored by  $\text{Cu}^{2+}$ , but varying levels of zinc are present, presumably due to the various origins of the copper. The variability of solid pyrochlore solutions with very different proportions of Sn and Sb is also evident, ‘pure’ tin yellow being rare.

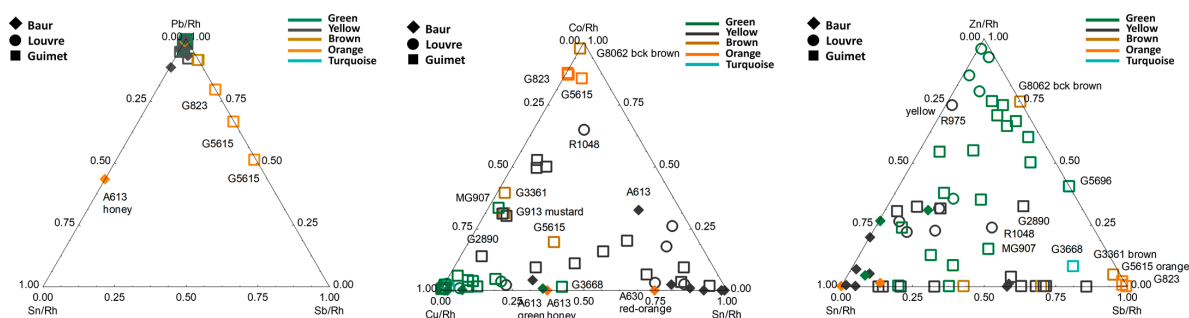


**Figure 11.** Comparison of the signal of elements associated with the yellow, green/turquoise, and brown/orange colored areas (normalized with Rh signal).

## 6. Conclusions

This study demonstrates the potential of on-site and completely non-invasive analysis to compare enameling technologies. The complementarity of pXRF and mobile Raman microspectrometry is obvious. Although the analysis is made from the surface on a heterogeneous material, the procedure of visualization of the results makes it possible to classify the enamels according to the elementary ratios and therefore to assign them to the raw materials. High efficiency is noted for the blue (and green) colors due to the different geological contexts of the cobalt sources in Asia and Europe—more work on the characterization of cobalt ores is needed to progress further—especially for the yellow and green colors due to the complex non-stoichiometry of the pyrochlore pigment (tin yellow-Naples yellow).

The procedure is also efficient in distinguishing between the different nanoparticles used to prepare pigments from rose to violet colors. The comparison of the elements present in the marks is also very instructive to detect posterior addition. Unfortunately, the molecular techniques used here cannot identify the use of borax (which would be possibly achievable by PIGE or by Raman using blue laser excitation) nor fluxes as sodium (measured by SEM-EDS, PIXE and PIGE) and lithium (PIGE) [33]. The comparison of the XRF signal levels relative to yttrium, rubidium and strontium signals is particularly effective to identify the use of European raw materials. The cobalt-manganese-nickel and cobalt-manganese-arsenic diagrams differentiate the sources of cobalt and help to date the period of production. The combined Raman -pXRF procedure makes it possible to assess for each color of each artefact the degree of use of local raw materials and those which are imported.

**Supplementary Materials:** The following supporting information can be downloaded at: <https://www.mdpi.com/article/10.3390/ceramics6010026/s1>, Table S1: XRF Guimet data; Table S2: XRF Louvre data.

**Author Contributions:** Conceptualization, P.C.; methodology, P.C. and G.S.F.; investigation, X.G., J.B. and P.C.; resources, B.Z. and J.-B.C.; writing—original draft preparation, P.C. and G.S.F.; writing—review and editing, P.C., G.S.F., J.B., B.Z. and J.-B.C. All authors have read and agreed to the published version of the manuscript.

**Funding:** The research in France was partially funded by the French *Agence Nationale de la Recherche* ANR EnamelFC project—19-CE27-0019-02.

**Institutional Review Board Statement:** Not applicable.

**Informed Consent Statement:** Not applicable.

**Data Availability Statement:** All data given as Supplementary Materials.

**Acknowledgments:** Museum direction and staff are cordially thanked for their support and their authorization to study the artifacts. Ludovic Bellot-Gurlet (Monaris, Paris), Claire Delery (mnaa-Guimet) and Pauline d’Abrigeon (Baur Fondation, Musée d’arts d’Extrême-Orient, Genève) are kindly acknowledged for many discussions as well as Mathieu Lebon (MNHN) for the availability of XRF instrument.

**Conflicts of Interest:** The authors declare no conflict of interest.

## References

- Colomban, P.; Sagon, G.; Faurel, X. Differentiation of antique ceramics from the Raman spectra of their coloured glazes and paintings. *J. Raman Spectrosc.* **2001**, *32*, 351–360. [CrossRef]
- Colomban, P. Glazes and Enamels. In *Encyclopedia of Glass Science, Technology, History, and Culture*; Richet, P., Ed.; J. Wiley & Sons Inc.: New York, NY, USA, 2020; Ch.10.6. Available online: <https://www.wiley.com/en-us/Encyclopedia+of+Glass+Science%2C+Technology%2C+History%2C+and+Culture%2C+2+Volume+Set-p-9781118799499> (accessed on 15 September 2022).
- Colomban, P. Glass, Pottery and enamelled objects: Identification of their technology and origin. In *Conservation Science—Heritage Materials*; Garside, P., Richardson, E., Eds.; The Royal Society of Chemistry: Cambridge, UK, 2019; Chapter 7; pp. 200–247.
- Epler, R.A.; Epler, D.R. *Glazes and Glass Coatings*; The American Ceramic Society: Westerville, OH, USA, 2000.
- Fraser, H. *Glazes for the Craft Potter, Revised Edition*; A&C Black: London, UK; The American Ceramic Society: Westerville, OH, USA, 1998.
- Colomban, P.; Simsek Franci, G.; Kirmızı, B. Cobalt and Associated Impurities in Blue (and Green) Glass, Glaze and Enamel: Relationships between Raw Materials, Processing, Composition, Phases and International Trade. *Minerals* **2021**, *11*, 633. [CrossRef]
- Neri, E.; Morvan, C.; Colomban, P.; Guerra, M.F. Late Roman and Byzantine mosaic opaque ‘glass-ceramics’ tesserae (5th–9th century). *Ceram. Int.* **2016**, *42*, 18859–18869. [CrossRef]
- d’Albis, A. *Traité de la Porcelaine de Sèvres*; Fatou: Dijon, France, 2003.
- Munier, P. *Technologie des Faïences*; Gauthier-Villars: Paris, France, 1957.
- Colomban, P.; Zhang, Y.; Zhao, B. Non-invasive Raman analyses of *huafalang* and related porcelain wares. Searching for evidence for innovative pigment technologies. *Ceram. Int.* **2017**, *43*, 12079–12088. [CrossRef]
- Colomban, P.; Kirmızı, B.; Zhao, B.; Clais, J.-B.; Yang, Y.; Droguet, V. Non-invasive on-site Raman study of pigments and glassy matrix of the 17th–18th century painted enamelled Chinese metal wares: Comparison with French enamelling technology. *Coatings* **2020**, *10*, 471. [CrossRef]
- Colomban, P.; Gironde, M.; Vangu, D.; Kirmızı, B.; Zhao, B.; Cochet, V. The technology transfer from Europe to China in the 17th–18th centuries: Non-invasive on-site XRF and Raman analyses of Chinese Qing Dynasty enameled masterpieces made using European ingredients/recipes. *Materials* **2021**, *14*, 7434. [CrossRef]
- Colomban, P.; Kirmızı, B.; Zhao, B.; Clais, J.-B.; Yang, Y.; Droguet, V. Investigation of the Pigments and Glassy Matrix of Painted Enamelled Qing Dynasty Chinese Porcelains y Noninvasive On-Site Raman Microspectrometry. *Heritage* **2020**, *3*, 915–941. [CrossRef]
- Burlot, J.; Bellot-Gurlet Vangu, D.; Colomban, P. Naples yellow pyrochlores and related pigments: A Raman signature of enameling technology traced by PCA, full-range and band-by-band fitting. *J. Raman Spectrosc.* **2023**. *submitted*.
- Colomban, P.; Simsek Franci, G.; Gironde, M.; d’Abrigeon, P.; Schumacher, A.-C. pXRF Data Evaluation Methodology for On-site Analysis of Precious Artifacts: Cobalt used in the Blue Decoration of Qing Dynasty Overglazed Porcelain enameled at Custom District (Guangzhou), Jingdezhen and Zaobanchu (Beijing) workshops. *Heritage* **2022**, *5*, 1752–1778. [CrossRef]
- Colomban, P.; Gironde, M.; Simsek Franci, G.; d’Abrigeon, P. Distinguishing Genuine Imperial Qing Dynasty Porcelain from Ancient Replicas by On-site Non-invasive XRF and Raman Spectroscopy. *Materials* **2022**, *15*, 5747. [CrossRef]
- Simsek Franci, G. Blue Print: Archaeometric Studies of Colored Glazed Chinese Ceramics and Production of Replica, Final Report, The Scientific and Research Council of Turkey, The Scientific and Technological Projects Funding Program. Unpublished Report. 3 January 2021.
- Simsek Franci, G. Handheld X-ray Fluorescence (XRF) versus wavelength dispersive XRF: Characterization of Chinese blue and white porcelain sherds using handheld and laboratory-type XRF instruments. *Appl. Spectrosc.* **2020**, *74*, 314–322. [CrossRef] [PubMed]
- Simsek, G.; Colomban, P.; Wong, S.; Zhao, B.; Rougeulle, A.; Liem, N.Q. Toward a fast non-destructive identification of pottery: The sourcing of 14th–16th century Vietnamese and Chinese ceramic shards. *J. Cult. Herit.* **2015**, *16*, 159–172. [CrossRef]
- Liu, H.W.; Wang, H.; Duan, P.Q.; Gao, H.; Zhang, R.; Qu, L. The Qianlong Emperor’s order: Scientific analysis helps find French painted enamel among Palace Museum collections. *Heritage Sci.* **2022**, *10*, 132. [CrossRef]
- Kingery, W.D.; Vandiver, P.B. The Eighteenth-Century Change in Technology and Style from the *Famille-Verte* Palette to the *Famille-Rose* Palette. In *Technology and Style*; Kingery, W.D., Ed.; Ceramics and Civilization Series; The American Ceramic Society: Columbus, OH, USA, 1986; Volume 2, pp. 363–381.
- Van Pevenage, J.; Lauwers, D.; Herremans, D.; Verhaeven, E.; Vekemans, B.; de Clercq, W.; Vincze, L.; Moens, L.; Vandenabeele, P. A combined spectroscopic study on Chinese porcelain containing ruan-cai colours. *Anal. Meth.* **2014**, *6*, 6387–6394. [CrossRef]
- Li, Y.Q.; Zhu, J.; Ji, L.Y.; Shan, Y.Y.; Jiang, S.; Chen, G.; Sciau, P.; Wang, W.X.; Wang, C.S. Study of Arsenic in *Famille Rose* Porcelain from the Imperial Palace of Qing Dynasty, Beijing, China. *Ceram. Int.* **2018**, *44*, 1627–1632. [CrossRef]
- Duan, H.Y.; Zhang, X.Q.; Kang, B.Q.; Wang, G.Y.; Qu, L.; Lei, Y. Non-Destructive Analysis and Deterioration Study of a Decorated *Famille Rose* Porcelain Bowl of Qianlong Reign from the Forbidden City. *Stud. Conserv.* **2019**, *64*, 311–322. [CrossRef]
- Giannini, R.; Freestone, I.C.; Shortland, A.J. European cobalt sources identified in the production of Chinese *famille rose* porcelain. *J. Archaeol. Sci.* **2017**, *80*, 27–36. [CrossRef]



26. Wang, Q.; Chin, L.; Wang, C. *Underglaze Blue and Red: Elegant Decoration on Porcelain of Yuan, Ming and Qing*; Multi-Art: Hong Kong, China, 1993.
27. Norris, D.E.; Braekmans, D.; Domoney, K.; Shortland, A. The Composition and Technology of Polychrome Enamels on Chinese Ruby-Backed Plates Identified Through Nondestructive Micro-X-ray Fluorescence. *X-ray Spectrom.* **2020**, *49*, 502–510. [CrossRef]
28. Miao, J.; Yang, B.; Mu, D. 2010. Identification and Differentiation of Opaque Chinese Overglaze Yellow Enamels by Raman Spectroscopy and Supporting Techniques. *Archaeometry* **2001**, *52*, 146–155. [CrossRef]
29. Norris, D.E.; Braekmans, D.; Shortland, A. Technological connections in the development of 18th and 19th century Chinese painted enamels. *J. Archaeol. Sci. Rep.* **2022**, *42*, 103406. [CrossRef]
30. Colomban, P.; Gironde, M.; Edwards, H.G.M.; Mesqui, V. The enamels of the first (softpaste) European blue-and-white porcelains: Rouen, Saint-Cloud and Paris factories: Complementarity of Raman and X-ray fluorescence analyses with mobile instruments to identify the cobalt ore. *J. Raman Spectrosc.* **2021**, *52*, 2246–2261. [CrossRef]
31. Colomban, P.; Ngo, A.-T.; Fournery, N. Non-invasive Raman Analysis of 18th Century Chinese Export/Armorial Overglazed Porcelain: Identification of the Different Enameling Technology. *Heritage* **2022**, *5*, 233–259. [CrossRef]
32. Colomban, P.; Ambrosi, F.; Ngo, A.-T.; Lu, T.-A.; Feng, X.-L.; Chen, S.; Choi, C.-L. Comparative analysis of *wucaï* Chinese porcelains using mobile and fixed Raman microspectrometers. *Ceram. Int.* **2017**, *43*, 14244–14256. [CrossRef]
33. Burlot, J.; Colomban, P.; Bellot-Gurlet, L.; Lemasson, Q. PIGE and PIXE evidence of the use of lithium-rich borax in Chinese and European 18th century enamel. *J. Eur. Cer. Soc. Submitted*.
34. Montanari, R.; Murakami, N.; Alberghina, M.F.; Pelosi, C.; Schiavone, S. The Origin of overglaze-blue enameling in Japan: New discoveries and a reassessment. *J. Cult. Herit.* **2019**, *37*, 94–102. [CrossRef]
35. Landry-Deron, I. Les Mathématiciens envoyés en Chine par Louis XIV en 1685. In *Archive for History of Exact Sciences*; Springer: Berlin/Heidelberg, Germany, 2001; pp. 423–463.
36. Loehr, G. Missionary-artists at the Manchu Court. *Trans. Orient. Ceram. Soc.* **1963**, *34*, 51–67. Available online: <https://www.orientalceramicsociety.org.uk/publications/transactions/4> (accessed on 2 June 2022).
37. Shih, C.-F. Evidence of East-West exchange in the eighteenth century: The establishment of painted enamel art at the Qing Court in the reign of Emperor Kangxi. *Natl. Palace Mus. Res. Q.* **2007**, *24*, 45–94.
38. Xu, X.D. Europe-China-Europe: The Transmission of the Craft of Painted Enamel in the Seventeenth and Eighteenth Centuries. In *Goods from the East, 1600–1800 Trading Eurasia*; Berg, M., Gottmann, F., Hodacs, H., Nierstrasz, C., Eds.; Palgrave Macmillan: London, UK, 2015; pp. 92–106.
39. Palace Museum. *Treasures from Oversea Countries, Exhibition Catalogue of Kulangsu Gallery of Foreign Artefacts from the Palace Museum Collection*; Gugong Chubanshe: Beijing, China, 2011.
40. Kleutghen, K. Chinese Occidenterie: The Diversity of “Western” Objects in Eighteenth-Century China. *Eighteenth-Century Stud.* **2014**, *47*, 117–135. [CrossRef]
41. de Rochebrunne, M.L. Les porcelaines de Sèvres envoyées en guise de cadeaux diplomatiques à l’empereur de Chine par les souverains français dans la seconde moitié du XVIII<sup>e</sup> siècle. *Extrême-Orient Extrême-Occident* **2019**, *43*, 81–92. [CrossRef]
42. Finlay, J. Henri Bertin and Louis XV’s Gifts to the Qianlong Emperor. *Extrême-Orient Extrême-Occident* **2019**, *43*, 93–112. [CrossRef]
43. Guo, F. Presents and Tribute: Exploration of the Presents Given to the Qianlong Emperor by the British Macartney Embassy. *Extrême-Orient Extrême-Occident* **2019**, *43*, 143–172. [CrossRef]
44. Ma, H.J.; Henderson, J.; Cui, J.F.; Chen, K.L. Glassmaking in the Qing Dynasty: A Review, New Data, and New Insights. *Adv. Archaeomater.* **2020**, *1*, 27–35. [CrossRef]
45. Curtis, E.B. Aspects of a multi-faceted process: The circulation of enamel wares between the Vatican and Kangxi’s court. *Extrême-Orient Extrême-Occident* **2020**, *43*, 29–39. [CrossRef]
46. Xu, Y. Painted Enamel on Ceramics. The Encounter on Dutch and Chinese Pottery. Available online: <https://www.aronson.com/painted-enamel-on-ceramic-the-encounter-of-dutch-and-chinese-pottery/> (accessed on 9 November 2022).
47. Wang, M.C.-P. Eighteenth-century Chinese Painted Enamelware Materials and Technique. *Fond. Baur Bull.* **2022**, *80*, 24–53.
48. Colomban, P.; Kirmızı, B.; Gougeon, C.; Gironde, M.; Cardinal, C. Pigments and glassy matrix of the 17th–18th century enamelled French watches: A non-invasive on-site Raman and pXRF study. *J. Cult. Herit.* **2020**, *44*, 1–14. [CrossRef]
49. Shih, C.-F. The Arrival of a New Colour Palette in Eighteenth-century Jingdezhen. In *Le Secret des Couleurs—Céramiques de Chine et d’Europe du XVIII<sup>e</sup> Siècle à nos Jours*; d’Abrigeon, P., Ed.; Fondation Baur-Musée des Arts d’Extrême-Orient: Genève, Switzerland, 2022; pp. 20–59.
50. Colomban, P.; Milande, V.; Lucas, H. On-site Raman analysis of Medici porcelain. *J. Raman Spectrosc.* **2004**, *35*, 68–72. [CrossRef]
51. Colomban, P.; Milande, V. On-site Raman analysis of the earliest known Meissen porcelain and stoneware. *J. Raman Spectrosc.* **2006**, *37*, 606–613. [CrossRef]
52. Wood, N. *Chinese Glazes: Their Origins, Chemistry and Recreation*; A & C Black: London, UK, 1999; pp. 194–195.
53. Kerr, R.; Wood, N. *Science and Civilisation in China: Volume 5, Chemistry and Chemical Technology*; Part 12, Ceramic Technology; Cambridge University Press: Cambridge, UK, 2004.
54. Wood, N. An AAS study of Chinese imperial yellow porcelain odies and their place in the history of Jingdezhen’s porcelain development. *Adv. Archaeomater.* **2021**, *2*, 49–65. [CrossRef]
55. Colomban, P.; Treppoz, F. Identification and differentiation of ancient and modern European porcelains by Raman macro- and micro-spectroscopy. *J. Raman Spectrosc.* **2001**, *32*, 93–102. [CrossRef]

56. d'Albis, A. Une remarquable tasse en rouge de cuivre réalisée à la Manufacture de Sèvres en 1848. In *Le Secret des Couleurs—Céramiques de Chine et d'Europe du XVIIIe siècle à nos jours*; d'Abrigeon, P., Ed.; Fondation Baur-Musée des Arts d'Extrême-Orient: Genève, Switzerland, 2022; pp. 131–135.
57. Maggetti, M.; d'Albis, A. Phase and compositional analysis of a Sèvres soft paste porcelain plate from 1781, with a review of early porcelain techniques. *Eur. J. Min.* **2017**, *29*, 347–367. [CrossRef]
58. Deck, T. *La Faïence*; Maison Quantin: Paris, France, 1887.
59. Menegon, E. Amicia Palatina: Les jésuites et la politique des cadeaux offerts à la Cour de Qing. *Extrême-Orient Extrême-Occident* **2019**, *43*, 61–80. [CrossRef]
60. National Palace Museum (Ed.) *Porcelain with Painted Enamels of Qing Yongzheng pPeriod (1723–1735)*; pl. 21, pl. 22; National Palace Museum: Taipei, Taiwan, 1879.
61. National Palace Museum (Ed.) *Special Exhibition of Ch'ing Dynasty Enamelled Porcelains of the Imperial Ateliers*; National Palace Museum: Taipei, Taiwan, 1992.
62. Jörg, C.J.A. *Porcelain and the Dutch China Trade*; Martinus Nijhoff: La Haye, NL, USA, 1982.
63. Cort, L.A.; Stuart, J. *Joined Colors: Decoration and Meaning in Chinese Porcelain*; Arthur M. Sackler Gallery, Smithsonian Institution/Tai Yip Co.: Whashington, DC, USA; Hong Kong, China, 1993.
64. Shih, C.-F. *Hua Falang: The Chinese Concept of Painted Enamels, in the RA Collections of Chinese Ceramics: A Collector's Vision*; Jorge Welsh Books: London, UK, 2001; Volume V, pp. 29–59.
65. Shih, C.-F. *Radiant Luminance: The Painted Enamelware of the Qing Imperial Court*; The National Palace Museum: Taipei, Taiwan, 2012.
66. *Catalogue Porcelain with Painted Enamels of Qing Period*; National Palace Museum: Taipei, Taiwan, 2013.
67. Colomban, P. The Discovery and Comparison of the Manufacturing Secrets of Enamelled Masterpieces. *Orientations* **2022**, *53*, 92–96. Available online: <https://www.orientations.com.hk/past-issues/p/janfeb-2022-1> (accessed on 9 November 2022).
68. Portable XRF Spectrometer. Available online: <https://xrfcheck.bruker.com/InfoDepth> (accessed on 6 July 2022).
69. Demirsar Arli, B.; Simsek Franci, G.; Kaya, S.; Arli, H.; Colomban, P. Portable X-ray Fluorescence (p-XRF) uncertainty estimation for glazed ceramic analysis: Case of Iznik Tiles. *Heritage* **2020**, *3*, 1302–1329. [CrossRef]
70. Burlot, J.; Gallet, X.; Simsek Franci, G.; Bellot-Gurlet, L.; Colomban, P. Non-Invasive On-Site pXRF Analysis of Coloring Agents of Under- and Over-Glazes: Variability and Representativity of Measurements on Porcelain. *Colorants* **2023**, *2*, 42–57. [CrossRef]
71. Sakellariou, K.; Miliani, C.; Morresi, A.; Ombelli, M. Spectroscopic investigation of yellow majolica glazes. *J. Raman Spectrosc.* **2004**, *35*, 61–67. [CrossRef]
72. Sandalinas, C.; Ruiz-Moreno, S. Lead-tin-antimony yellow-Historical manufacture, molecular characterization and identification in seventeenth-century Italian paintings. *Stud. Conserv.* **2004**, *49*, 41–52. [CrossRef]
73. Sandalinas, C.; Ruiz-Moreno, S.; Lopez-Gil, A.; Miralles, J. Experimental confirmation by Raman spectroscopy of a Pb-Sn-Sb triple oxide yellow pigment in sixteenth-century Italian pottery. *J. Raman Spectrosc.* **2006**, *37*, 1146–1153. [CrossRef]
74. Rosi, F.; Manuali, V.; Miliani, C.; Brunetti, B.G.; Sgamellotti, A.; Grygar, T.; Hradil, D. Raman scattering features of lead pyroantimonate compounds. Part I: XRD and Raman characterization of Pb<sub>2</sub>Sb<sub>2</sub>O<sub>7</sub> doped with tin and zinc. *J. Raman Spectrosc.* **2009**, *40*, 107–111. [CrossRef]
75. Ricciardi, P.; Colomban, P.H.; Tournié, A.; Milande, V. Non-destructive on-site identification of ancient glasses: Genuine artefacts, embellished pieces or forgeries? *J. Raman Spectrosc.* **2009**, *40*, 604–617. [CrossRef]
76. Pereira, M.; de Lacerda-Aroso, T.; Gomes, M.J.M.; Mata, A.; Alves, L.C.; Colomban, P. Ancient Portuguese ceramic wall tiles (“Azulejos”): Characterization of the glaze and ceramic pigments. *J. Nano Res.* **2009**, *8*, 79–88. Available online: <https://www.scientific.net/JNanoR.8.109> (accessed on 9 November 2022).
77. Pelosi, C.; Agresti, G.; Santamaria, U.; Mattei, E. Artificial yellow pigments: Production and characterization through spectroscopic methods of analysis. *e-Preserv. Sci.* **2010**, *7*, 108–115.
78. Rosi, F.; Manuali, V.; Grygar, T.; Bezdzicka, P.; Brunetti, B.G.; Sgamellotti, A.; Burgio, L.; Seccaroni, C.; Miliani, C. Raman scattering features of lead pyroantimonate compounds: Implication for the non-invasive identification of yellow pigments on ancient ceramics. Part II. In situ characterisation of Renaissance plates by portable micro-Raman and XRF studies. *J. Raman Spectrosc.* **2011**, *42*, 407–414. [CrossRef]
79. Cartechini, L.; Rosi, F.; Miliani, C.; D'Acapito, F.; Brunetti, B.G.; Sgamellotti, A. Modified Naples yellow in Renaissance majolica: Study of Pb-Sb-Zn and Pb-Sb-Fe ternary pyroantimonates by X-ray absorption spectroscopy. *J. Anal. At. Spectrom.* **2011**, *26*, 2500–2507. [CrossRef]
80. Pinto, A.; Sciau, P.; Zhu, T.Q.; Zhao, B.; Groenen, E.S. Raman study of Ming porcelain dark spots: Probing Mn-rich spinels. *J. Raman Spectrosc.* **2019**, *50*, 711–719. [CrossRef]
81. Porter, Y. Le cobalt dans le monde Iranien (IXe-XVIe siècles). *Taoci* **2000**, *1*, 5–14.
82. Matin, M.; Pollard, A.M. From ore to pigment: A description of the minerals and experimental study of cobalt ore processing from the Kāshān mine, Iran. *Archaeometry* **2017**, *59*, 731–746. [CrossRef]
83. Matin, M.; Pollard, A.M. Historical accounts of cobalt ore processing from the Kāshān mine, Iran. *Iran* **2015**, *53*, 171–183. [CrossRef]
84. Watt, J.C.Y. Notes on the use of cobalt in later Chinese ceramics. *Ars Orient.* **1979**, *11*, 63–85.

85. Wen, R.; Wang, C.S.; Mao, Z.W.; Huang, Y.Y.; Pollard, A.M. The chemical composition of blue pigment on Chinese blue-and-white porcelain of the Yuan and Ming Dynasties (AD 1271–1644). *Archaeometry* **2007**, *49*, 101–115. [\[CrossRef\]](#)
86. Huang, S.-Z. *Xi Yang Chao Gong Dian Lu (Registration of Taxes from Foreign Countries)*; Zhong wai jiao tong shi ji cong kan Series; Zhejiang Gongshang University Press: Hangzhou, China, 1520.
87. Medley, M. *The Chinese Potter. A Practical History of Chinese Ceramics*, 3rd ed.; Phaidon: London, UK, 1999.
88. Yu, K.N.; Miao, J.M. Non-destructive analysis of Jingdezhen Blue and White porcelains of the Ming dynasty using EDXRF. *X-ray Spectrom.* **1996**, *25*, 281–285. [\[CrossRef\]](#)
89. Colomban, P.; Liem, N.Q.; Sagon, G.; Tinh, H.X.; Hoành, T.B. Microstructure, composition and processing of 15th century Vietnamese porcelains and celadons. *J. Cult. Herit.* **2003**, *4*, 187–197. [\[CrossRef\]](#)
90. Yap, C.T.; Tang, S.M. X-ray fluorescence analysis of modern and recent Chinese porcelains. *Archaeometry* **1984**, *26*, 78–81. [\[CrossRef\]](#)
91. Yap, C.T. A quantitative spectrometric analysis of trace concentrations of manganese and cobalt in ceramics and the significance of As/Co and Mn/Co ratios. *J. Archaeol. Sci.* **1988**, *15*, 173–177. [\[CrossRef\]](#)
92. Yu, K.N.; Miao, J.M. Locating the origins of blue and white porcelains using EDXRF. *Appl. Radiat. Isot.* **1997**, *48*, 959–963. [\[CrossRef\]](#)
93. Yu, K.N.; Miao, J.M. Multivariate analysis of the energy dispersive X-ray fluorescence results from blue and white Chinese porcelains. *Archaeometry* **1998**, *40*, 331–339. [\[CrossRef\]](#)
94. Yu, K.N.; Miao, J.M. Characterization of blue and white porcelains using Mn/Fe ratio from EDXRF, with particular reference to porcelains of the Xuande period (1426 to 1435 A.D.). *Appl. Radiat. Isot.* **1999**, *51*, 279–283. [\[CrossRef\]](#)
95. Morimoto, A.; Yamasaki, K. *Technical Studies on Ancient Ceramics Found in North and Central Vietnam*; Fukuoka Museum: Fukuoka, Japan, 2001.
96. Cheng, H.S.; Zhang, B.; Xia, H.N.; Jiang, J.C.; Yang, F.J. Non-destructive analysis and appraisal of ancient Chinese porcelain by PIXE. *Nucl. Instr. Meth. Phys. Res. Sect. B* **2002**, *190*, 488–491. [\[CrossRef\]](#)
97. Colomban, P.; Calligaro, T.; Vibert-Guigue, C.; Nguyen, N.Q.; Edwards, H.G.M. Dorures des céramiques et tesselles anciennes: Technologies et accrochage. *ArchéoSciences* **2005**, *29*, 7–20. [\[CrossRef\]](#)
98. Bertran, H.; Reboulleau, M.; Magnier, R.; Romain, A. *Nouveau Manuel Complet de la Peinture sur Verre, sur Porcelaine et sur Émail*; Encyclopédie-Roret, L., Ed.; Mulo: Paris, France, 1913.
99. Simsek, G.; Colomban, P.; Casadio, F.; Bellot-Gurlet, L.; Zelleke, G.; Faber, K.T.; Milande, V.; Tilliard, L. On-site Identification of Early Böttger Red Stoneware using portable XRF/Raman Instruments: 2, Glaze and Gilding Analysis. *J. Am. Ceram. Soc.* **2015**, *98*, 3006–3013. [\[CrossRef\]](#)
100. Zhang, F.K. The origin and development of traditional Chinese glazes and decorative ceramics color. In *Ancient Technology to Modern Science, Ceramics and Civilization*; Kingery, W.D., Ed.; The American Ceramic Society: Westerville, OH, USA, 1984; Volume 1, pp. 163–180.
101. Yang, Y.M.; Feng, M.; Ling, X.; Mao, Z.Q.; Wang, C.S.; Sun, X.M.; Guo, M. Microstructural analysis of the color-generating mechanism in Ru ware, modern copies and its differentiation with Jun ware. *J. Archaeol. Sci.* **2005**, *32*, 301–310. [\[CrossRef\]](#)
102. Kingery, W.D.; Vandiver, P.B. Song Dynasty Jun (Chung) ware glazes. *Am. Ceram. Bull.* **1983**, *62*, 1269–1274.
103. Freestone, I.C.; Barber, D.J. The development of the colour of sacrificial red glaze with special reference to a Qing Dynasty saucer dish. In *Chinese Copper Red Wares*; Scott, R.E., Ed.; Percival David Foundation of Chinese Art, Monograph Series n°3; University of London, School of Oriental and African Art: London, UK, 1992; pp. 53–62.
104. Sciau, P.; Noé, L.; Colomban, P. Metal nanoparticles in contemporary potters' master pieces: Lustre and red 'pigeon lood' potteries as models to understand the ancient pottery. *Ceram. Int.* **2016**, *42*, 15349–15357. [\[CrossRef\]](#)
105. Hunt, L.B. The True Story of Purple of Cassius Gold Bull. *Gold Bull.* **1976**, *9*, 134–139. [\[CrossRef\]](#)
106. Colomban, P. The Use of Metal Nanoparticles to Produce Yellow, Red and Iridescent Colour, from bronze Age to Present Times in Lustre Pottery and Glass: Solid State Chemistry, Spectroscopy and Nanostructure. *J. Nano Res.* **2009**, *8*, 109–132.
107. Geyssant, J. Secret du verre rouge transparent de Bernard Perrot et comparaison avec celui de Johann Kunckel. In *Bernard Perrot (1640–1709), Secrets et Chefs-d'œuvre des Verreries Royales d'Orléans, Catalogue*; Klinka Ballesteros, I., de Valence, C., Maitte, C., Rieke, H., Eds.; Musée des Beaux-Arts d'Orléans—SOMOGY Editions d'Arts: Paris, France, 2013; pp. 51–54.
108. Colomban, P.; Kirmizi, B. Non-invasive on-site Raman study of polychrome and white enamelled glass artefacts in imitation of porcelain assigned to Bernard Perrot and his followers. *J. Raman Spectrosc.* **2020**, *51*, 133–146. [\[CrossRef\]](#)
109. d'Abrigeon, P. (Ed.) *Le Secret des Couleurs—Céramiques de Chine et d'Europe du XVIIIe Siècle à nos Jours*; Fondation Baur-Musée des Arts d'Extrême-Orient: Genève, Switzerland, 2022.
110. Tang, H. Colour Matters: The Consumption of Overglaze enameled Wares in Eighteenth-century Europe. In *Le Secret des Couleurs—Céramiques de Chine et d'Europe du XVIIIe siècle à nos jours*; d'Abrigeon, P., Ed.; Fondation Baur-Musée des Arts d'Extrême-Orient: Genève, Switzerland, 2022; pp. 65–73.

**Disclaimer/Publisher's Note:** The statements, opinions and data contained in all publications are solely those of the individual author(s) and contributor(s) and not of MDPI and/or the editor(s). MDPI and/or the editor(s) disclaim responsibility for any injury to people or property resulting from any ideas, methods, instructions or products referred to in the content.